

AD-A111 067 AIR FORCE INST OF TECH WRIGHT-PATTERSON AFB OH SCHOO--ETC F/G 22/3

ACTIVE CONTROL OF LINEAR PERIODIC SYSTEMS.(U)

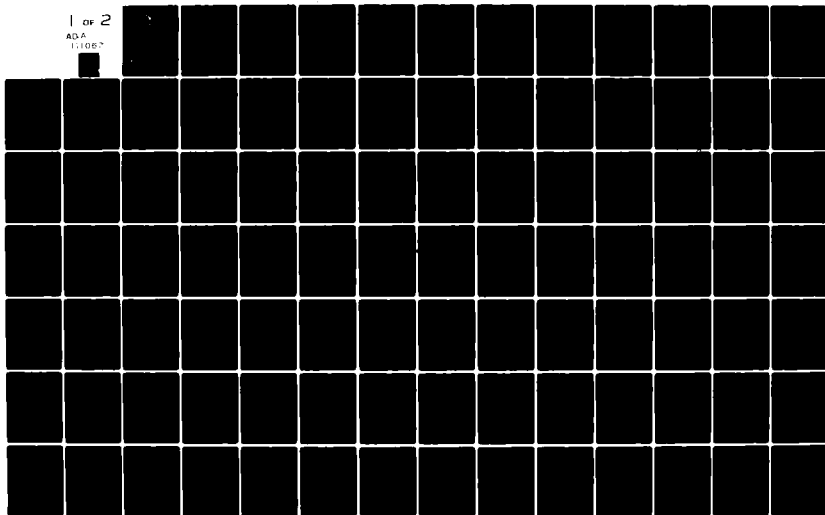
DEC 81 6 5 YEAKEL

UNCLASSIFIED AFIT/GA/AA/81D-12

NL

1 of 2

ADA
111067



AD A111067



LEVEL II

① fw

DTIC
ELECTE
FEB 18 '82

S

D

E



DTIC FILE COPY

DEPARTMENT OF THE AIR FORCE
AIR UNIVERSITY (ATC)
AIR FORCE INSTITUTE OF TECHNOLOGY

Wright-Patterson Air Force Base, Ohio

This document has been approved
for public release and sale; its
distribution is unlimited.

82 02 18 061

LEVEL II

①

AFIT/GA/AA/81D-12

ACTIVE CONTROL OF LINEAR
PERIODIC SYSTEMS
THESIS

AFIT/GA/AA/81D-12

Glenn S. Yeakel
1st Lt USAF

Approved for public release; distribution unlimited

AFIT/GA/AA/81D-12

ACTIVE CONTROL OF LINEAR
PERIODIC SYSTEMS

THESIS

Presented to the Faculty of the School of Engineering
of the Air Force Institute of Technology
Air University (ATC)
in Partial Fulfillment of the
Requirements for the Degree of
Master of Science

Accession For	
NTIS GRAB	<input checked="checked" type="checkbox"/>
DTIC IAB	<input type="checkbox"/>
Unannounced	<input type="checkbox"/>
Justified	<input type="checkbox"/>
By _____	
Dist _____	
Av. _____	
Dist _____	
A	

by

Glenn S. Yeakel, B.S.

1st Lt USAF

Graduate Astronautics

December 1981

Approved for public release; distribution unlimited

Preface

With this thesis, I hope to help open the book on understanding the behavior and the means of controlling periodic systems. Many problems in the field of astronautics deal with periodic systems and as we stand on the brink of the exploitation of outer space, I feel we need more understanding of these periodic systems.

I would like to extend my appreciation to my advisor, Dr. Robert Calico. With his insight and knowledge I was able to overcome many problems encountered during the course of this study.

Also, I would like to thank my wife Donna. No study of this magnitude is without its sleepless nights, periods of enlightenment and times of frustration. She experienced these times with me and never once displayed dissatisfaction over the fact that I was not with her in thought while at home.

Finally, I would like to dedicate this report to my father, who passed away during its final preparation. It was the values he instilled within me that made me able to finish this task.

G. Scott Yeakel

Table of Contents

	Page
Preface	ii
List of Figures	v
List of Tables.	vii
List of Notations	viii
Abstract.	x
I Introduction.	1
Background.	1
Problem and Scope	5
II Problem Analysis.	6
Satellite Attitude Kinematics	6
Symmetric Satellite in an Elliptical Orbit.	9
Unsymmetric Satellite in a Circular Orbit	16
III Floquet Theory.	25
Periodic Systems.	25
Floquet Theory.	25
IV Control Theory.	31
Modal Control Theory.	31
Mode Controllability Matrix	35
Control Law	37
Control Law Implementation.	39
Single Controlled Mode	40
Multiple Controlled Modes.	45
V Results	48

	Page
Test Cases.	48
Stability Analysis.	49
Satellite Stabilization and Verification. . .	65
Single Mode Stabilization.	65
Multiple Controlled Mode Stabilization . .	67
Numerical Problems Associated with	
$F^{-1}(\tau)$ Computation.	87
VI Concluding Remarks and Recommendations.	92
Bibliography.	95

List of Figures

Figure		Page
1	Basic Layout of Two-Body Orbit.	7
2	Uncontrolled $x_1(\tau)$ Response for Case 2.	52
3	Uncontrolled $x_2(\tau)$ Response for Case 2.	53
4	Uncontrolled $x_3(\tau)$ Response for Case 2.	54
5	Uncontrolled $x_4(\tau)$ Response for Case 2.	55
6	Uncontrolled First Mode Response for Case 2	57
7	Uncontrolled Second Mode Response for Case 2.	58
8	Uncontrolled Third Mode Response for Case 2	59
9	Uncontrolled Fourth Mode Response for Case 2.	60
10	Uncontrolled First Mode Response for Case 3	61
11	Uncontrolled Second Mode Response for Case 3.	62
12	Uncontrolled Third Mode Response for Case 3	63
13	Uncontrolled Fourth Mode Response for Case 3.	64
14	Controlled System First Mode Response for Case 1.	68
15	Controlled System Second Mode Response for Case 1	69
16	Controlled System Third Mode Response for Case 1.	70
17	Controlled System Fourth Mode Response for Case 1	71
18	Controlled System First Mode Response for Case 4.	74
19	Controlled System Second Mode Response for Case 4	75
20	Controlled System Third Mode Response for Case 4.	76
21	Controlled System Fourth Mode Response for Case 4	77
22	Controlled $x_1(\tau)$ Response for Case 4.	78
23	Controlled $x_2(\tau)$ Response for Case 4.	79

Figure		Page
24	Controlled $x_3(\tau)$ Response for Case 4.	80
25	Controlled $x_4(\tau)$ Response for Case 4.	81
26	Controlled System First Mode Response for Case 5. .	83
27	Controlled System Second Mode Response for Case 5 .	84
28	Controlled System Third Mode Response for Case 5. .	85
29	Controlled System Fourth Mode Response for Case 5 .	86
30	$F^{-1}(\tau)$ Calculated at $\tau = \pi$ using the Fourier Coefficients and Analytical Techniques.	91

List of Tables

Table		Page
I	Non-zero Coefficient Matrix Elements for the Symmetric Satellite.	15
II	Non-zero Coefficient Matrix Elements for the Unsymmetric Satellite.	21
III	Parametric Values of the Five Test Cases	49
IV	Characteristic Exponents of the Five Test Cases. .	50
V	Case 1 Characteristic Exponents with $K = (-2.0, 0.0, 0.0, 0.0)$	66
VI	Case 4 Characteristic Exponents with $K = (4.0, -10.0, 0.0, 0.0)$	72
VII	Case 5 Characteristic Exponents with $K = (-1.4, 0.0, -.01, 0.0)$	82
VIII	Theoretical and Computed Values of the Characteristic Exponents for Case 3.	89

List of Notation

English

$A(\tau)$	Coefficient matrix of linear system
$B(\tau)$	Applications matrix of control term
$F(\tau)$	Partitioned matrix made up of the eigenvectors
I	Mass moment of inertia matrix
J	Jordan form matrix
K	Gain matrix of control term
M	External moment vector
$R(\tau)$	Mode-controllability matrix of the control term
$\bar{f}_i(\tau)$	Eigenvector of linear system
k_i	Inertia ratios
$u(\tau)$	Control law
$\bar{x}(\tau)$	State vector of linear system

Script

a	Semi-major axis of orbit
e	Orbital eccentricity
r	Orbital range between body and satellite

Greek

Δ	Constant true anomaly rate for circular orbit
T	Period
$\Phi(\tau)$	State transition matrix
α	Spin parameter
ζ	non-dimensional range
$\bar{n}(\tau)$	Modal coordinate vector
θ_i	Euler angles of satellite body

Greek (cont)

λ_i	Characteristic exponent
μ	Gravitational Parameter
v	True anomaly
ρ_i	Eigenvalue of monodromy matrix
τ	Non-dimensional time
$\bar{\omega}$	Angular velocity
$\dot{\omega}$	Angular acceleration

Abstract

The linearized equations describing the attitude motion of two generic satellite cases are developed. In both cases, the symmetric satellite in an elliptical orbit and an unsymmetric satellite in a circular orbit, the linearized equations are periodic. Using Floquet theory, the stability of the attitude motion for several satellite designs is checked. For satellites with unacceptable attitude stability, an active control scheme utilizing modal control design techniques is developed. With this control scheme, various satellite test cases are stabilized and the results are verified via a digital simulation of the satellite attitude motion.

CHAPTER I

INTRODUCTION

Background

With the advent of artificial satellites in the late 1950's, satellite designers have sought various methods to control the orientation of satellite bodies. The need for proper attitude, or line of sight, control is evident when one looks at the various missions that satellites perform. Whether a satellite is performing a space surveillance mission for one of the 'super-powers' or providing a communications link for a third world country, the proper attitude must be maintained at all times to assure the satellite is accomplishing its intended functions. A simple example is a reconnaissance satellite in a low earth orbit at an altitude of two hundred miles. If the line of sight of the cameras on board this satellite is perturbed by as little as five degrees, the camera will miss its desired aimpoint by approximately seventeen miles. This is totally inadequate performance for the surveillance of a battlefield with high resolution cameras.

To control the attitude of satellites, satellite designers have used several devices ranging from passive techniques using gravity gradient stabilization to active devices using control moment gyros, dual spin configurations, magnetic torquers, or gyrocompasses. A desirable feature

of gravity gradient stabilization is that gravity torque stabilizes the satellite in lieu of a torque producing device. Since no torque device, and its necessary control equipment, is required, the satellite is less costly to build and to launch. However, there are some serious drawbacks to gravity gradient stabilization, which include restricted satellite designs and low eccentricity orbits (Ref. 8: 199). These two restrictions cause problems with the physical design of satellites and their intended missions. In addition to these restrictions, the natural frequency of oscillation of a stable gravity gradient satellite is very low, and precise attitude control is not attainable by this means alone.

In the 1960's, as the use of satellites increased and the exploitation of space with unmanned vehicles began, this general problem of attitude stability of satellites under the influence of a gravity gradient was recognized. Two papers published in the 1960's dealt with the topic of attitude stability of spinning satellites under the influence of a gravity gradient torque. The first paper examined the attitude stability of unsymmetric satellites in circular orbits (Ref. 6: 114). In their study, Kane and Shippey examined satellite attitude motion and derived linearized equations with periodic coefficients. Since the linearized equations had periodic coefficients, their asymptotic stability was determined by using Floquet theory. In fact, the stability of this class of satellites was

determined to be a function of moment of inertia ratios and spin rates (Ref. 6: 114-119). In the second study, Kane and Barba examined the stability of symmetric satellites in elliptical orbits. Like the first study, this study provided a periodic linear system model of the satellite attitude motion. Once again, Floquet theory was used to determine the stability of this class of satellites. During this study, stability was found to be dependent on the spin rate and moment of inertia ratios like the first study, and on the orbital eccentricity (Ref. 7: 402-405). These two studies were concerned exclusively with the passive stability of the satellite attitude; there was no attempt to control these satellites because of the non-constant coefficients of the linearized systems.

The results of these two studies provided valuable information for satellite engineers in the 1960's and 1970's. However, as we become more and more dependent on satellites and find new uses for satellites, we may no longer be able to satisfy the requirements for passive stabilization or we may simply want to increase the low damping of the natural low frequency oscillations. In fact, with the advent of the Space Transportation System, many space planners are developing concepts of large space structures for use in the future. One of the general mission requirements of these large space structures is precise vehicle line of sight stability (Ref. 4: 52). With this requirement, considering that low orbital eccentricities, spin rates, and vehicle design requirements need to

be overcome, an active control scheme for these satellites must be developed. However, a problem arises in the development of an active controller for these satellites. The linear systems used to model the attitude dynamics of both the unsymmetric satellite in a circular orbit and the symmetric satellite in an elliptical orbit are nonautonomous, or specifically periodic, systems. As such, these systems do not allow the use of classical linear controller design techniques.

The control of periodic systems is a topic which is in need of further research. Many references can be found on the control of constant coefficient linear systems. However, very little material can be found on periodic systems as well as the control of such systems. In his study in 1980, Shelton (Ref. 14) found modal control techniques feasible to control the orbit of a satellite in orbit about the third libration point, where the orbit is a time-periodic system. Therefore, since this type of control methodology was used to control a time-periodic system, it is used in this study for the control of satellite attitude motion.

Modal control is a modern control technique which attempts to independently control systems modes by means of providing state feedback which is proportional to the eigenvectors of the dual basis for the system. Using direct feedback of the modal variables, the closed-loop eigenvalues of a constant coefficient system can be placed at a desired location using pole placement techniques. Also, when a con-

stant coefficient system is controlled, the time response of the system can be controlled directly through the gain selection. In this study, modal control techniques are used to control the location, in the complex plane, of the characteristic exponents. These characteristic exponents, of both the open and closed-loop systems, are found using Floquet theory.

Problem and Scope

The problem addressed by this study is the control of linear systems with periodic coefficients. Shelton developed a controller for a particular periodic system in his research. However, the system he addressed had one unstable characteristic exponent. To handle this system, he developed a simplified controller to control only one mode. In this study, the general form of a controller capable of controlling any number of modes is developed. This general controller is implemented in several example cases and the results are verified by the use of a digital simulation of the linearized closed-loop system.

CHAPTER II

PROBLEM ANALYSIS

The major thrust of this study is to develop a control scheme for the use with linear periodic systems. As mentioned previously, the two periodic systems of interest are the symmetric satellite in an elliptical orbit and the unsymmetric satellite in a circular orbit. In this chapter, the attitude dynamics of these two satellite cases are examined. With these results, the linearized equations for the satellite attitude motion are developed.

Satellite Attitude Kinematics

The first step in developing the equations of motion for the attitude dynamics of a satellite is the derivation of the kinematics of the problem. This step involves the establishment of coordinate frames, angular displacements, and angular rates. As depicted in Figure 1, the basic orbital layout consists of a satellite S orbiting body F , with an assumed inertial frame at F . Additionally, r and v , which represent the range and true anomaly of the satellite, are the polar coordinates of S with respect to F .

The angular orientation of satellite S in inertial space is found through a series of rotations. The first rotation to Frame 1 is a rotation equal to the true anomaly about the \hat{k}_1 unit vector. Subsequent rotations to a body-fixed frame are: a rotation of θ_1 about the \hat{i}_1 axis,

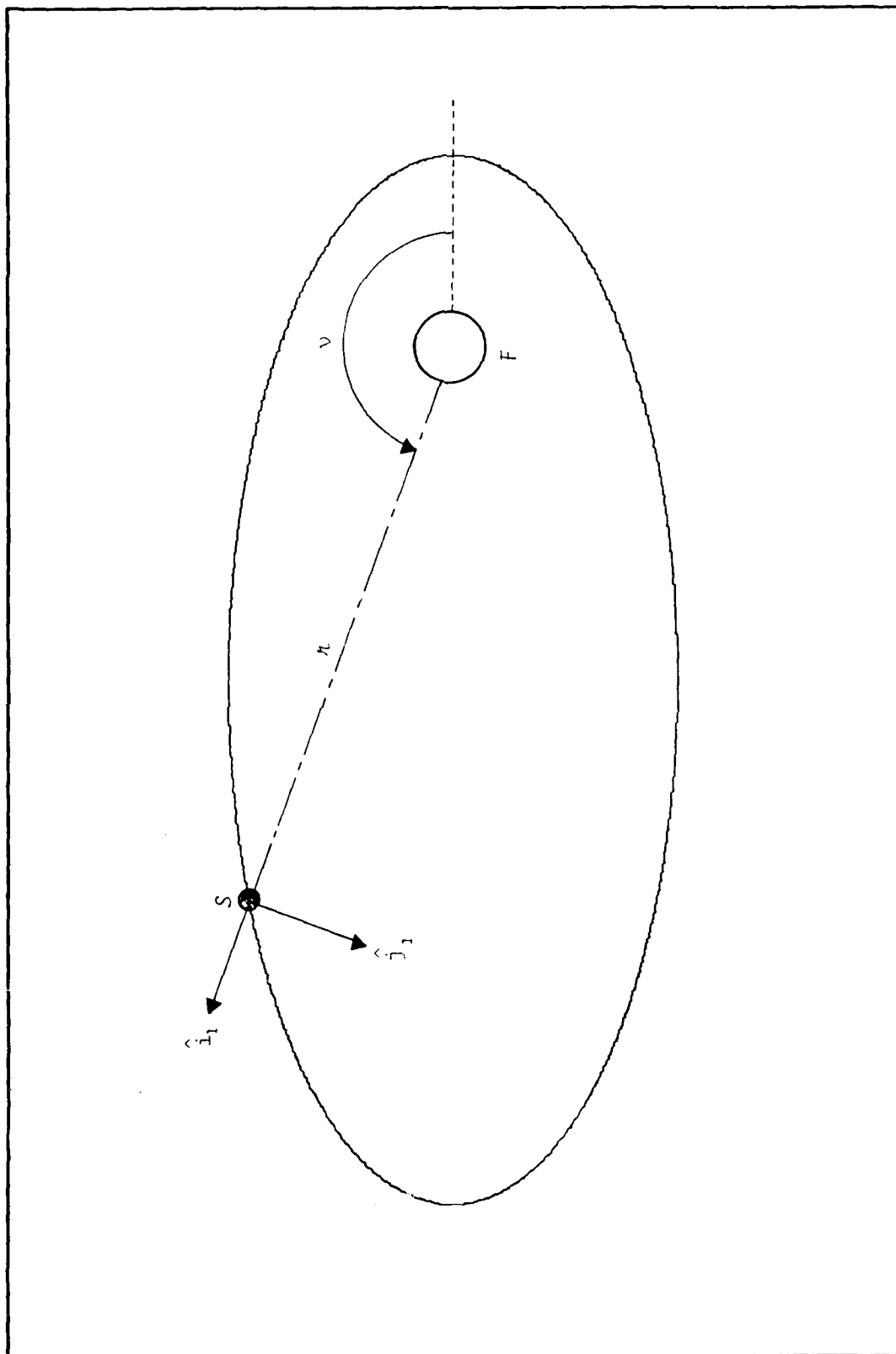


Figure 1. Basic Layout of Two-Body Orbit

a rotation of θ_2 about the \hat{j}_2 axis, and a rotation of θ_3 about the \hat{k}_3 axis. These angles, θ_1 , θ_2 , and θ_3 , represent the pitch, roll, and yaw of the satellite body.

With these angular rotations, the total angular velocity and acceleration of S with respect to inertial space can be determined. By using the angular velocity chain rule,

$$\bar{\omega}^4|i = \bar{\omega}^4|_3 + \bar{\omega}^3|_2 + \bar{\omega}^2|_1 + \bar{\omega}^1|i \quad (1)$$

the angular velocity is found,

$$\bar{\omega}^4|i = \dot{\theta}_3 \hat{k}_3 + \dot{\theta}_2 \hat{j}_3 + \dot{\theta}_1 \hat{i}_1 + \dot{\psi} \hat{k}_1 \quad (2)$$

Using the proper coordinate transformations, the angular velocity in frame 3 may be written as

$$\{\bar{\omega}^4|i\} = \begin{bmatrix} \dot{\theta}_1 \cos \theta_2 - \dot{\psi} \cos \theta_1 \sin \theta_2 \\ \dot{\theta}_2 + \dot{\psi} \sin \theta_1 \\ \dot{\theta}_3 + \dot{\theta}_1 \sin \theta_2 + \dot{\psi} \cos \theta_1 \cos \theta_2 \end{bmatrix}_3 \quad (3)$$

where the subscript provides the reference axis system.

Through the use of the vector differential rule,

$$\frac{d}{dt} \bar{\omega}^4|i = \frac{d}{dt} \bar{\omega}^4|i + \bar{\omega}^3|i \times \bar{\omega}^4|i \quad (4)$$

the angular acceleration, $\ddot{\omega}^4|i$, is found,

$$\{\ddot{\omega}^i\} = \begin{bmatrix} \ddot{\theta}_1 \cos \theta_2 - \dot{\theta}_1 \dot{\theta}_2 \sin \theta_2 - \ddot{\nu} \cos \theta_1 \sin \theta_2 + \dot{\theta}_2 \dot{\theta}_3 + \ddot{\nu} \\ (-\ddot{\theta}_2 \cos \theta_1 \cos \theta_2 + \dot{\theta}_1 \sin \theta_1 \sin \theta_2 + \dot{\theta}_2 \sin \theta_1) \\ \ddot{\theta}_2 + \ddot{\nu} \sin \theta_1 + \dot{\theta}_1 \dot{\theta}_2 \cos \theta_1 - \dot{\theta}_3 \dot{\theta}_1 \cos \theta_2 + \dot{\theta}_3 \dot{\theta}_2 \cos \theta_1 \\ \cos \theta_2 \\ \ddot{\theta}_1 \sin \theta_2 + \dot{\theta}_1 \dot{\theta}_2 \cos \theta_2 + \ddot{\nu} \cos \theta_2 \cos \theta_1 + \dot{\theta}_3 - \ddot{\nu} \\ (\dot{\theta}_2 \sin \theta_2 \cos \theta_1 + \dot{\theta}_1 \cos \theta_2 \sin \theta_1) \end{bmatrix} \quad (5)$$

With these two vectors, the angular velocity and angular acceleration of S with respect to inertial space, the equations for the satellite attitude dynamics can be derived.

Symmetric Satellite in an Elliptical Orbit

(Ref. 7: 402-404)

The development of the equations of motion for the attitude of a symmetric satellite in an elliptical orbit perturbed by a gravity gradient torque is given by Kane and Barba (1966). The following derivation is adopted from this reference.

The first step in this development is the investigation of the orbital motion of a satellite in the common two-body orbit, Figure 1. In addition to the parameters specified in Figure 1, the orbital eccentricity is noted as e , and a is the semi-major axis of the orbit. In the polar coordinates r and ν , the differential equations describing the two-body orbit are,

$$\ddot{r} - r\dot{\nu}^2 + \frac{\mu}{r^2} = 0 \quad (6a)$$

and

$$r^2 \dot{\nu} = \sqrt{a\mu}(1-e^2)^{1/2} \quad (6b)$$

where μ is the Gravitational Parameter. The two-body satellite motion is periodic, and the period may be found from Kepler's Second Law (Ref. 1: 33):

$$T = \frac{2\pi}{\sqrt{\mu}} a^{3/2} \quad (7)$$

With this result, Equation (6) can be rewritten

$$\ddot{r} - \mu \dot{\theta}^2 + \left(\frac{2\pi}{T}\right)^2 \frac{a^3}{r^2} = 0 \quad (8a)$$

and

$$\mu \dot{\theta}^2 = \frac{2\pi}{T} a^2 (1-e^2)^{1/2} \quad (8b)$$

Substituting (8b) into (8a), one obtains a differential equation for the range of a satellite, in an elliptical orbit, from the central body:

$$\ddot{r} - r \left[\frac{2\pi}{T} \frac{a^2}{r^2} (1-e^2)^{1/2} \right]^2 + \left(\frac{2\pi}{T}\right)^2 \frac{a^3}{r^2} = 0 \quad (9)$$

This differential equation can be nondimensionalized by making the following variable transformations:

$$\tau = \frac{2\pi}{T} t \quad \zeta = \frac{r}{a}$$

where τ and ζ represents nondimensional time and distance, respectively. With these nondimensional variables, Equation (9) becomes

$$\zeta'' + \frac{1}{\zeta^2} + \frac{(e^2-1)}{\zeta^3} = 0 \quad (10)$$

where the prime indicates derivatives with respect to τ . The resulting Equation (10) is a second order differential equation. As such, it requires two initial conditions: Assuming that the satellite begins at perigee,

$$r_{\text{perigee}} = a(1-e)$$

$$\dot{r}_{\text{perigee}} = 0$$

the initial conditions for equation (10) are

$$r(0) = 1-e$$

$$\dot{r}(0) = 0$$

At this point, the equations of motion for the satellite attitude can be derived using Euler's Moment Equation:

$$\{M\}_3 = [I]_3 \left\{ \frac{d}{dt} \bar{\omega}^4 | i \right\}_3 + \{\bar{\omega}^3 | i\}_3 [I]_3 \{\bar{\omega}^4 | i\}_3 \quad (11)$$

where $[I]$ is the mass moment of inertia tensor

$[\bar{\omega}]$ is the skew matrix associated with $\bar{\omega}^3 | i$, and

$\{M\}$ is the external moment vector.

Assuming that the axes are defined in such a way that Frame 3 lies along the principal axes of the satellite body, the inertia tensor takes the form

$$[I] = \begin{bmatrix} I_{11} & [0] \\ & I_{22} \\ [0] & & I_{33} \end{bmatrix} \quad (12)$$

Additionally, the skew symmetric matrix associated with angular velocity has the form

$$[\bar{\omega}^3 | i] = \begin{bmatrix} 0 & -\omega_3 & \omega_2 \\ \omega_3 & 0 & -\omega_1 \\ -\omega_2 & \omega_1 & 0 \end{bmatrix} \quad (13)$$

where ω_1 , ω_2 , and ω_3 are the individual components of $\bar{\omega}^3 | i$.

Substituting Equations (3), (5), (12), and (13) into Equation (11) produces moment equations in the form:

$$\{M\} = \begin{bmatrix} I_{11}\omega'_1 + (I_{33} - I_{22})\omega_2\omega_3 \\ I_{22}\omega'_2 + (I_{11} - I_{33})\omega_1\omega_3 \\ I_{33}\omega'_3 + (I_{22} - I_{11})\omega_1\omega_2 \end{bmatrix} \quad (14)$$

where the external moments on S by body F are (Ref. 7: 403),

$$\{M\} = \begin{bmatrix} 3\left(\frac{2\pi}{T}\right)^2 \zeta^{-3} \begin{matrix} 0 \\ I_{11} - I_{33} \end{matrix} \cos\theta_2 \sin\theta_2 \\ 0 \end{bmatrix}_3 \quad (15)$$

Equating Equations (14) and (15), recalling that for a symmetric satellite, $I_{11} = I_{22}$, one finds

$$\begin{bmatrix} I_{11}\omega'_1 + (I_{33} - I_{22})\omega_2\omega_3 = 0 \\ I_{11}\omega'_2 + (I_{11} - I_{33})\omega_1\omega_3 = 3\left(\frac{2\pi}{T}\right)^2 \zeta^{-3} (I_{11} - I_{33}) \cos\theta_2 \sin\theta_2 \\ \omega'_3 = 0 \end{bmatrix} \quad (16)$$

Finally, by defining an inertia parameter k_1 such that

$$k_1 = \frac{I_{33} - I_{22}}{I_{11}}$$

Equation (16) becomes

$$\begin{aligned} \omega'_1 + k_1 \omega_2 \omega_3 &= 0 \\ \omega'_2 - k_1 \omega_1 \omega_3 + \frac{3}{\zeta^3} \left(\frac{2\pi}{T}\right)^2 k_1 \cos\theta_2 \sin\theta_2 &= 0 \\ \omega'_3 &= 0 \end{aligned} \quad (17)$$

The three nonlinear differential equations given by Equation (17) can be combined with Equation (3) to obtain three second order equations in the variables θ_1 , θ_2 , and θ_3 .

By defining the state vector to be

$$\bar{x}(\tau) = \begin{bmatrix} \vartheta_1(\tau) \\ \vartheta_2(\tau) \\ \vartheta_1'(\tau) \\ \vartheta_2'(\tau) \end{bmatrix}$$

and noting the reference state,

$$\bar{x}_0 = \bar{0}$$

a linear system of the form

$$\bar{x}'(\tau) = A(\tau)\bar{x}(\tau)$$

can be derived in the neighborhood of the reference state.

To obtain this linear system, the original system

$$\bar{x}'(\tau) = \bar{f}[\bar{x}(\tau)]$$

is linearized about \bar{x}_0 such that

$$A_{ij} = \left. \frac{\partial f_i}{\partial x_j} \right|_{\bar{x} = \bar{x}_0} \quad i, j = 1, \dots, 4$$

The resulting coefficient matrix, A , is a function of the inertia parameter, k_1 , and the variables, ϑ' , ϑ'' , and ϑ_3' . To produce a usable linear system, the dependence on these variables must be eliminated. The dependence on ϑ' and ϑ'' can be eliminated through the use of Equation (8b). From Equation (8b),

$$\vartheta' = \frac{2\pi}{T} \frac{a^2}{h^2} (1-e^2)^{1/2} \quad (18)$$

and by nondimensionalizing with ξ and τ , one obtains

$$\vartheta' = \frac{(1-e^2)^{1/2}}{C^2} \quad (19)$$

which by differentiation with respect to τ yields,

$$v'' = \frac{-2(1-e^2)^{1/2}}{\zeta^3} \zeta' \quad (20)$$

Replacing v' and v'' with Equations (19) and (20) eliminates the dependence on these variables. To eliminate the dependence on θ'_3 , one recognizes from Equation (16)

$$\omega'_3 = 0$$

implying that

$$\omega_3 = v' + \theta'_3 = \text{constant}$$

The dependence on θ'_3 is eliminated by specifying this constant. However, the constant ω_3 represents the spin rate of the satellite and the true anomaly rate. Since one is concerned only with the spin rate of the satellite, the constant is defined as $(\alpha + 1)$ and

$$v' + \theta'_3 = (\alpha + 1) \quad (21)$$

Substituting Equations (19) through (21) into the linearized coefficient matrix, a linear equation is found in the form of

$$\bar{x}'(\tau) = A(\tau) \bar{x}(\tau)$$

where $A(\tau)$ is explicitly a function of ζ and implicitly a function of τ . The individual elements of this coefficient matrix for the linearized system are presented in Table 1.

Upon examining Table I, one notes the coefficient matrix is a function of the orbital eccentricity, the spin parameter, the inertia parameter, ζ and ζ' . Since ζ repre-

Table I
Non-Zero Coefficient Matrix Elements
for the Symmetric Satellite

$$A(1,3) = 1$$

$$A(2,4) = 1$$

$$A(3,1) = \frac{(1-e^2)}{\zeta^4} - \frac{(1+\alpha)}{\zeta^2} (1+k_1) (1-e^2)^{1/2}$$

$$A(3,2) = \frac{-2(1-e^2)^{1/2}}{\zeta^3} \zeta'$$

$$A(3,4) = \frac{2(1-e^2)^{1/2}}{\zeta^3} - (1+\alpha) (1+k_1)$$

$$A(4,1) = \frac{2(1-e^2)^{1/2}}{\zeta^3} \zeta'$$

$$A(4,2) = \frac{(1-e^2)}{\zeta^4} - \frac{(1+\alpha)}{\zeta^2} (1+k_1) (1-e^2)^{1/2} - \frac{3k_1}{\zeta^3}$$

$$A(4,3) = (1+\alpha) (1+k_1) - \frac{2(1-e^2)^{1/2}}{\zeta^2}$$

sents the nondimensional distance from the satellite to body F , it is periodic with the same period as the orbital period. Thus,

$$z(\tau) = z(\tau + T)$$

where $T = 2\pi$ and since A is a function of z

$$A(\tau) = A(\tau + T) \quad (22)$$

Thus, the equations for the attitude motion of the symmetric satellite are periodic and this periodicity is due to the orbital motion of the satellite.

Unsymmetrical Satellite in a Circular Orbit

(Ref. 6: 114-117)

The development of the equations describing the attitude motion for the unsymmetric satellite in a circular orbit perturbed by gravity gradient torque are given by Kane and Shippey (1963), from which the following derivation is adopted.

Unlike the symmetric satellite, this case does not require analyzing the orbital motion. Therefore, the first step in the derivation is to employ Euler's Moment Equation (11). In this case, since the satellite is not symmetric the body fixed axes are used as the reference frame. Using coordinate transformations, Equation (3) can be written as

$$\{\ddot{\omega}^4/i\} = \begin{bmatrix} (\ddot{\theta}_1 \cos \theta_2 - \dot{\nu} \cos \theta_1 \sin \theta_2) \cos \theta_3 + \\ (\ddot{\theta}_2 + \dot{\nu} \sin \theta_1) \sin \theta_3 \\ (\ddot{\theta}_2 + \dot{\nu} \sin \theta_1) \cos \theta_3 - (\ddot{\theta}_1 \cos \theta_2 - \\ \dot{\nu} \sin \theta_2 \cos \theta_1) \sin \theta_3 \\ \ddot{\theta}_3 + \ddot{\theta}_1 \sin \theta_2 + \dot{\nu} \cos \theta_2 \cos \theta_1 \end{bmatrix} \quad (23)$$

Since the attitude of the satellite in this case, like the symmetric satellite, is a function of θ_1 and θ_2 , only small angles are considered. Considering only small angles, Equation (23) can be linearized about these small angles by using the following approximations:

$$\begin{aligned} \cos \theta_1 &\approx 1 & \sin \theta_1 &\approx \theta_1 \\ \cos \theta_2 &\approx 1 & \sin \theta_2 &\approx \theta_2 \end{aligned} \quad (24)$$

Linearizing Equation (23), one obtains

$$\{\ddot{\omega}^4/i\} = \begin{bmatrix} (\ddot{\theta}_1 - \dot{\nu} \theta_2) \cos \theta_3 + (\ddot{\theta}_2 + \dot{\nu} \theta_1) \sin \theta_3 \\ (\ddot{\theta}_2 + \dot{\nu} \theta_1) \cos \theta_3 - (\ddot{\theta}_1 - \dot{\nu} \theta_2) \sin \theta_3 \\ \ddot{\theta}_3 + \dot{\nu} \end{bmatrix} \quad (25)$$

Since the orbit is circular, $\dot{\nu}$ is constant and $\ddot{\nu}$ is zero, for all time. Denoting $\dot{\nu}$ as Δ , the angular acceleration is found from Equation (25):

$$\{\ddot{\omega}^4/i\} = \begin{bmatrix} (\ddot{\theta}_1 - \Delta\dot{\theta}_2)\cos\theta_3 - (\dot{\theta}_1 - \Delta\theta_2)\sin\theta_3\dot{\theta}_3 + \\ (\ddot{\theta}_2 + \Delta\dot{\theta}_1)\sin\theta_3 + (\dot{\theta}_2 + \Delta\theta_1)\cos\theta_3\dot{\theta}_3 \\ -(\ddot{\theta}_1 - \Delta\dot{\theta}_2)\sin\theta_3 - (\dot{\theta}_1 - \Delta\theta_2)\cos\theta_3\dot{\theta}_3 + \\ (\ddot{\theta}_2 + \Delta\dot{\theta}_1)\cos\theta_3 - (\dot{\theta}_2 + \Delta\theta_1)\sin\theta_3\dot{\theta}_3 \\ \ddot{\theta}_3 \end{bmatrix} \quad (26)$$

From Kane and Shippy (Ref. 6: 114), the gravitational torque moments acting on S (linearized by using the small angle approximations of Equation (24)) are:

$$\{M\} = \begin{bmatrix} 3\Delta^2(I_{22} - I_{33})\dot{\theta}_2\sin\theta_3 \\ 3\Delta^2(I_{11} - I_{33})\dot{\theta}_2\cos\theta_3 \\ 3\Delta^2(I_{11} - I_{22})\sin\theta_3\cos\theta_3 \end{bmatrix} \quad (27)$$

With the Euler's Moment Equation (11) along with Equations (25) through (27) and the following inertia parameters:

$$k_1 = \frac{I_{33} - I_{22}}{I_{11}} \quad k_2 = \frac{I_{11} - I_{33}}{I_{22}} \quad k_3 = \frac{I_{22} - I_{11}}{I_{33}}$$

The equations describing the attitude motion are given by:

$$\begin{aligned} \sin\theta_3 \{ 4k_1\Delta^2\ddot{\theta}_2 + \ddot{\theta}_2 - \dot{\theta}_1\dot{\theta}_3(1+k_1) + \Delta\dot{\theta}_1(1-k_1) + \Delta\dot{\theta}_3\dot{\theta}_2 \\ (1+k_1) \} + \cos\theta_3 \{ \ddot{\theta}_1 - \Delta\dot{\theta}_1(1+k_1) + \dot{\theta}_2\dot{\theta}_3(1+k_1) + \Delta\theta_1\dot{\theta}_3 \\ (1+k_1) + k_1\Delta^2\ddot{\theta}_1 \} = 0 \end{aligned} \quad (28a)$$

$$\begin{aligned} \sin\theta_3 \{ -\ddot{\theta}_1 + \Delta\dot{\theta}_2(1+k_2) - \dot{\theta}_2\dot{\theta}_3(1-k_2) - \Delta\theta_1\dot{\theta}_3(1-k_2) \\ + k_2\Delta^2\ddot{\theta}_1 \} + \cos\theta_3 \{ -4\Delta^2k_2\ddot{\theta}_2 - \dot{\theta}_1\dot{\theta}_3(1-k_2) + \ddot{\theta}_2 + \Delta\theta_1 \\ (1+k_2) + \Delta\theta_2\dot{\theta}_3(1-k_2) \} = 0 \end{aligned} \quad (28b)$$

$$\ddot{\theta}_3 - 3\Delta^2 k_3 \sin\theta_3 \cos\theta_3 = 0 \quad (28c)$$

Defining a parameter, p ; such that

$$p^2 = -3\Delta^2 \frac{(k_1 + k_2)}{1+k_1 k_2^2} \quad (28d)$$

Equation (28c) becomes

$$\ddot{\theta}_3 + p^2 \sin\theta_3 \cos\theta_3 = 0 \quad (29)$$

This second-order differential equation for $\theta_3(t)$ contains a first integral

$$\dot{\theta}_3 = \pm \left[\frac{p^2}{2} (\cos 2\theta_3 - 1) + \theta^2 \right]^{1/2} \quad (30)$$

where

$$\theta = \theta_3(t=0)$$

Defining a new independent variable, τ , such that

$$\tau = 2\theta_3 \quad (31)$$

Equation (30) can be rewritten

$$\dot{\theta}_3 = \pm \left[\frac{p^2}{2} (\cos \tau - 1) + \theta^2 \right]^{1/2} \quad (32)$$

At this point, the linearized equations describing the attitude motion can be obtained. By defining the state vector:

$$\bar{x}(\tau) = \begin{bmatrix} \theta_1 \\ \theta_2 \\ \dot{\theta}_1 / \Delta \\ \dot{\theta}_2 / \Delta \end{bmatrix} \quad (33)$$

and a function β , such that

$$\beta = \frac{\lambda}{\theta_3} \quad (34)$$

a linear system of the form of

$$\tilde{x}'(\tau) = A(\tau)\tilde{x}(\tau)$$

is found. The differential equation for $x_1(\tau)$ and $x_2(\tau)$ are found by using Equation (31), (33), and (34):

$$x_1'(\tau) = \frac{E}{2} x_3(\tau)$$

and likewise,

$$x_2'(\tau) = \frac{B}{2} x_4(\tau)$$

The differential equations for $x_3(\tau)$ and $x_4(\tau)$ are found from linear combinations of Equations (28a) and (28b). The resulting coefficient matrix is given in Table II.

The function β can be found from Equations (28d), (32), and (34) such that

$$\beta = + \left[\frac{-3}{2} \frac{(k_1 + k_2)}{(1 + k_1 k_2)} (\cos \tau - 1) + \frac{\theta^2}{\Delta^2} \right]^{-1/2} \quad (35)$$

With this relation, all elements of Table II are functions of the independent variable τ .

Table II
Non-Zero Coefficient Matrix Elements
for the Unsymmetric Satellite

$$A(1,3) = \frac{\beta}{2}$$

$$A(2,4) = \frac{\beta}{2}$$

$$A(3,1) = -.5 + \frac{\beta+1}{4} [k_2(1-\cos\tau) - k_1(1+\cos\tau)]$$

$$A(3,2) = -\frac{(4\beta+1)}{4} (k_1+k_2) \sin \tau$$

$$A(3,3) = \frac{\beta+1}{4} (k_1+k_2) \sin \tau$$

$$A(3,4) = \frac{\beta-1}{2} + \frac{\beta+1}{4} [k_2(1-\cos\tau) - k_1(1+\cos\tau)]$$

$$A(4,1) = -\frac{(\beta+1)}{4} (k_1+k_2) \sin \tau$$

$$A(4,2) = -.5 + \frac{4\beta+1}{4} [k_2(1+\cos\tau) - k_1(1-\cos\tau)]$$

$$A(4,3) = -\frac{(\beta-1)}{4} - \frac{\beta+1}{4} [k_2(1+\cos\tau) - k_1(1-\cos\tau)]$$

$$A(4,4) = -\frac{(\beta+1)}{4} (k_1+k_2) \sin \tau$$

By examining Table 11, it is apparent that all elements are periodic with period τ , such that

$$\Lambda(\tau) = \Lambda(\tau + T)$$

where $T = 2\pi$.

Examining the elements of the coefficient matrix in Table 11, one notes the dependence of $\Lambda(\tau)$ on the three dimensionless parameters k_1 , k_2 , and β . The parameters k_1 and k_2 are specified by the size, shape, and mass distribution of S . The parameter β , however, is dependent on the independent variable τ and on $\dot{\theta}^2/\Delta^2$, which is a measure of the rotational rate of the satellite. The value of $\dot{\theta}^2/\Delta^2$ can be found for a particular satellite configuration and spin rate. Defining a spin parameter, α , and a parameter, k , such that

$$\alpha = \frac{\overline{\dot{\theta}_3}}{\Delta} \quad k^2 = \frac{p^2}{\dot{\theta}^2} \quad (36)$$

where $\overline{\dot{\theta}_3}$ is the average value of $\dot{\theta}_3$ during one revolution of S , the value of $\dot{\theta}^2/\Delta^2$ can be found for any value of α . Rewriting Equation (32) such that

$$\ddot{\theta}_3 = \pm \left[\frac{k^2 \dot{\theta}^2}{2} (\cos\tau - 1) + \dot{\theta}^2 \right]^{1/2} \quad (37)$$

and by using the method of separation of variables and the identity,

$$\frac{1}{2} (\cos\tau - 1) = -\sin^2\tau$$

Equation (37) can be rewritten

$$\pm \theta_3 dt = \frac{d\theta_3}{(1 - k^2 \sin^2 \tau)^{1/2}} \quad (38)$$

Defining T as the time required for θ_3 to change by an amount of 2π radians, Equation (38) can be written

$$\int_0^{2\pi} \frac{d\theta_3}{(1 - k^2 \sin^2 \tau)^{1/2}} = \pm \int_0^T \theta_3 dt \quad (39)$$

where the left hand side of Equation (39) is in the form of complete elliptic integral of the first kind. Performing the integrations, one finds

$$4\Omega(k) = \pm T \theta_3 \quad (40)$$

Since $\overline{\theta_3}$ is an average value during one revolution,

$$\overline{\theta_3} = \pm \frac{2\pi}{T} = \frac{\pi \theta}{2\Omega(k)}$$

and

$$\alpha = \frac{\pi \theta}{2\Omega(k)}$$

or

$$\frac{\theta}{\Delta} = \frac{2\Omega(k)\alpha}{\pi} \quad (41)$$

Thus, given a desired α , the parameter θ/Δ can be found from Equation (41) by finding k and then $\Omega(k)$. Substituting Equations (41) and (28d) into Equation (36), one obtains

$$\Omega(k)k = \pm \frac{\pi}{2\alpha} \left[\frac{-3(k_1 + k_2)}{1 + k_1 k_2} \right]^{1/2} \quad (42)$$

which yields a transcendental equation in terms of k . Solving this transcendental equation for $\Omega(k)$, Equation (41) and (35) can be used to solve for the function β to complete the solution of the $A(\tau)$ matrix calculations in Table II.

This completes the analysis of the unsymmetric satellite in a circular orbit around body F . A linear periodic system of equations was found with a period of 2π . Unlike the first case, where the periodicity is due to the elliptical orbital motion, the periodicity for this case is due to the rotation of the satellite about its body fixed \hat{k}_u axis.

CHAPTER III

FLOQUET THEORY

Periodic Systems

In Chapter II of this study, the linearized equations describing the attitude motion for the two satellite cases are derived. For both cases, the equations of motion are found to be linear of the form,

$$\bar{\mathbf{x}}'(\tau) = \mathbf{A}(\tau)\bar{\mathbf{x}}(\tau) \quad (43a)$$

where the coefficient matrix, $\mathbf{A}(\tau)$ is periodic such that

$$\mathbf{A}(\tau) = \mathbf{A}(\tau + T) \quad (43b)$$

with T being defined as the period of the linear system.

For periodic systems of this type the stability can be determined through the use of Floquet theory. The essence of Floquet theory allows equations in the form of Equation (43) to be theoretically reduced to the case of constant coefficient equations (Ref. 5: 60).

Floquet Theory

In general, Floquet theory states that the fundamental matrix for ordinary differential equations in the form of Equation (43) is given by

$$\Phi(\tau) = \mathbf{P}(\tau)e^{\Gamma\tau} \quad (44)$$

where Γ is a constant matrix and $\mathbf{P}(\tau)$ is a periodic matrix with the same period, T , as the coefficient matrix, $\mathbf{A}(\tau)$

(Ref. 12: 265). This fundamental matrix is similar to the fundamental matrix

$$\psi(\tau) = F(\tau)e^{J\tau} \quad (45)$$

where $F(\tau) = F(\tau + T)$ and J is the Jordan form matrix associated with the matrix F . For the case where F has n distinct eigenvalues λ_i , the Jordan form matrix, J , is diagonal. The n linearly independent solution vectors making up $\psi(\tau)$ in this case have the form

$$\bar{x}_i(\tau) = \bar{f}_i(\tau)e^{\lambda_i\tau} \quad (46)$$

where the $\bar{f}_i(\tau)$ are the column vectors of $F(\tau)$. The eigenvalues, λ_i , of the matrix F , which are termed the characteristic exponents, determine the asymptotic stability of the linear system. Specifically, if all the characteristic exponents have negative real parts, the system described by Equation (43) is stable. If the eigenvalues of F are not distinct, the Jordan form matrix is block diagonal and, like the distinct case, stability is assured if all the eigenvalues have negative real parts. Therefore, the system stability can be determined from the λ_i 's. It remains to be shown how these characteristic exponents can be computed.

In order to compute the characteristic exponents and the periodic matrix $P(\tau)$, we consider the following. The principal fundamental matrix, or state transition matrix over one period, $\phi(T,0)$, referred to as the monodromy matrix, is determined from the solution to the general matrix differential equation:

$$\frac{d}{d\tau} [\Phi(\tau)] = A(\tau)\Phi(\tau) \quad (47)$$

with the initial conditions

$$\Phi(0) = [I]$$

The monodromy matrix for a linear system of the form of Equation (43) can be found by direct numerical integration of Equation (47). With the monodromy matrix, a general solution to Equation (43) at $\tau = T$ is given by

$$\bar{x}(T) = \Phi(T,0)\bar{x}(0) \quad (48)$$

where $\bar{x}(0)$ is the initial conditions vector. From Equation (46), the solution at $\tau = T$ corresponding to a specific value of λ_i is:

$$\bar{x}_i(T) = e^{\lambda_i T} \bar{f}_i(T) \quad (49)$$

with the initial condition vector given by:

$$\bar{x}_i(0) = \bar{f}_i(0) \quad (50)$$

Substituting Equations (49) and (50) into Equation (48) yields:

$$\Phi(T,0)\bar{f}_i(0) = e^{\lambda_i T} \bar{f}_i(T) \quad (51)$$

where due to the periodic nature of $\bar{f}_i(\tau)$,

$$\bar{f}_i(T) = \bar{f}_i(0)$$

Rearranging Equation (51),

$$\{\phi(T,0) - 1e^{\lambda_i T}\}\bar{f}_i(0) = \bar{0} \quad (52)$$

or

$$\{B - I\rho\}\bar{v} = \bar{0}$$

where ρ is an eigenvalue and \bar{v} is an associated eigenvector of matrix B . Therefore, by analogy, $e^{\lambda_i T}$ is an eigenvalue and $\bar{f}_i(0)$ is an eigenvector of the monodromy matrix. Thus, by evaluating the eigenstructure of the monodromy matrix, the characteristic multipliers, ρ_i , defined by,

$$\rho_i = e^{\lambda_i T} \quad (53)$$

are found. With these n characteristic multipliers, the characteristic exponents are found by,

$$\lambda_i = \frac{\ln \rho_i}{T} \quad (54)$$

Using these characteristic exponents, the Jordan form matrix, J , of Equation (45) is found such that (Ref. 12: 267):

$$J = \begin{bmatrix} \lambda_1 & & & & [0] \\ & \lambda_2 & & & \\ & & \ddots & & \\ & & & \ddots & \\ [0] & & & & \lambda_n \end{bmatrix} \quad (55)$$

In addition to finding the characteristic exponents and the Jordan form matrix, for a complete solution in the form of Equation (45), the $F(\tau)$ matrix must be found for all τ . Since $F(\tau)$ is periodic with period T , finding $F(\tau)$, $\tau \in (0, T)$, is equivalent to finding $F(\tau)$ over all τ . Defining a matrix $\phi(\tau)$ such that:

$$\phi(\tau) = [\bar{x}_1(\tau) : \bar{x}_2(\tau) : \dots : \bar{x}_n(\tau)] \quad (56)$$

where

$$\begin{aligned} \bar{x}_1(\tau) &= e^{\lambda_1 \tau} \bar{f}_1(\tau) \\ &\vdots \\ \bar{x}_n(\tau) &= e^{\lambda_n \tau} \bar{f}_n(\tau) \end{aligned}$$

a fundamental matrix is formed. Analogous to this matrix, we can form a square $n \times n$ matrix $F(\tau)$ such that:

$$F(\tau) = [\bar{f}_1(\tau) : \bar{f}_2(\tau) : \dots : \bar{f}_n(\tau)] \quad (57)$$

Substituting the matrices $F(\tau)$ and J into Equation (45), the fundamental matrix, as given by Equation (56), is found. Being a fundamental matrix, it follows the matrix differential equation given by Equation (47) such that:

$$\dot{\phi}(\tau) = F(\tau)e^{J\tau}$$

and

$$\frac{d}{d\tau}(\phi(\tau)) = F'(\tau)e^{J\tau} + F(\tau)Je^{J\tau} = A(\tau)F(\tau)e^{J\tau} \quad (58)$$

Multiplying by the inverse of the matrix $e^{J\tau}$, and simplifying, Equation (58) becomes

$$F'(\tau) = A(\tau)F(\tau) - F(\tau)J \quad (59)$$

where the initial condition matrix, $F(0)$, is given by the partitioned matrix,

$$F(0) = [\bar{f}_1(0) : \bar{f}_2(0) : \cdots : \bar{f}_n(0)] \quad (60)$$

Thus, $F(\tau)$ can be found by integrating the matrix differential Equation (59), over one period, with the initial conditions given by Equation (60).

With these evaluation of the Jordan Form matrix, J , and the eigenvector matrix, $F(\tau)$, all system information is found to complete a Floquet solution of the linear periodic system of Equation (43). In the following chapter, these results are used to develop a control law to provide active control for these periodic systems.

CHAPTER IV

CONTROL THEORY

In his thesis on the control of a satellite orbit, W.L. Shelton found that modal control techniques provided a feasible control scheme for time-periodic systems (Ref. 14). Basically, modal control techniques allow the control engineer to decouple the various system modes and control them individually. In essence, in a completely controllable constant coefficient system, the poles of the system can be placed where desired using full state feedback. With these pole placement techniques, the characteristics of each mode can be specified.

Even though any number of modes can be controlled using modal control techniques, Shelton's system had only one mode requiring control. Thus, the controller developed was simplified to handle one mode, which is not the general case. In general, one would like to control any number of modes simultaneously. As shown in Chapter V of this study, the two example satellite cases at times exhibit more than one unstable characteristic exponent, or mode. Therefore, a generalized controller capable of controlling multiple modes is required. In this chapter, the design and implementation of this generalized controller is presented.

Modal Control Theory

The basic theory behind modal control is that any

system can be decoupled into individual modes. These individual modes are determined by the characteristics of system poles. Therefore, if the system is fourth order, there are four modes. To decouple a system into its individual modes one needs to consider the mathematical properties of similarity matrices. Matrices J and A are said to be similar if

$$J = F^{-1}AF \quad (61)$$

where J, F, and A are constant n-by-n matrices with F being nonsingular. Since J and A have the same eigenvalues, this equation can be used for pole placement (Ref. 9: 61).

Furthermore, J can be chosen in its simplest form, the Jordan canonical form. For n distinct real eigenvalues of A, the Jordan form matrix has the structure,

$$J = \begin{bmatrix} \sigma_1 & & & \\ & \sigma_2 & & \\ & & \ddots & \\ & & & \sigma_n \end{bmatrix} \quad (62)$$

where the σ_i 's represent the eigenvalues. The F matrix required for this similarity transformation, consists of a partitioned matrix of the n eigenvectors of A:

$$F = [\tilde{f}_1 \cdot \tilde{f}_2 \cdot \cdot \cdot \tilde{f}_n] \quad (63)$$

where \bar{f}_i is the eigenvector associated with σ_i . Thus, with the F matrix given by Equation (63), the matrix J is found to be similar to the matrix A . Applying this concept, a constant coefficient system can be decoupled. Given the system,

$$\dot{\bar{x}}(t) = A\bar{x}(t) \quad (64)$$

the n modes can be decoupled by defining a new set of coordinates, $\bar{\eta}(t)$,

$$\bar{x}(t) = F\bar{\eta}(t) \quad (65)$$

Taking the derivative of Equation (65) with respect to the independent variable, t , one finds

$$\dot{\bar{x}}(t) = F\dot{\bar{\eta}}(t) \quad (66)$$

Substituting Equations (65) and (66) into the original system equation,

$$F\dot{\bar{\eta}}(t) = AF\bar{\eta}(t)$$

or

$$\dot{\bar{\eta}}(t) = F^{-1}AF\bar{\eta}(t) \quad (67)$$

Thus, if F is made up of the n eigenvectors of A ,

$$\dot{\bar{\eta}}(t) = J\bar{\eta}(t) \quad (68)$$

This resulting system, expressed in modal variable, consists of a set of n uncoupled differential equations:

$$\begin{aligned}
\dot{\eta}_1(t) &= \sigma_1 \eta_1(t) \\
\dot{\eta}_2(t) &= \sigma_2 \eta_2(t) \\
&\vdots \\
\dot{\eta}_n(t) &= \sigma_n \eta_n(t)
\end{aligned} \tag{69}$$

Since the eigenvalues of J and A are the same, the stability characteristics and responses of the individual modes has not changed. This same technique of decoupling the system modes can be applied to linear periodic systems in the form of Equation (43), using the results of Chapter III. However, since control of the system is desired, a control term must be added to the state equations.

Applying control to the system, the state equations in the form of Equation (43), are augmented with a control term,

$$\bar{x}'(\tau) = A(\tau)\bar{x}(\tau) + B(\tau)\bar{u}(\tau) \tag{70}$$

Where $\bar{u}(\tau)$ is the control vector and $B(\tau)$ is the applications matrix. The application matrix, $B(\tau)$, identifies the state variables to which $\bar{u}(\tau)$ is applied. Like the uncontrolled constant coefficient system, Equation (70) can be transformed into a set of uncoupled differential equations.

Defining modal variables, $\bar{\eta}(\tau)$, such that

$$\bar{x}(\tau) = F(\tau)\bar{\eta}(\tau)$$

Equation (70) can be rewritten

$$\begin{aligned}
F'(\tau)\bar{\eta}(\tau) + F(\tau)\bar{\eta}'(\tau) &= A(\tau)F(\tau)\bar{\eta}(\tau) + \\
&B(\tau)\bar{u}(\tau)
\end{aligned} \tag{71}$$

Simplifying this result, a set of differential equations for the modal variables is found,

$$\begin{aligned}\dot{\tilde{\eta}}'(\tau) = F^{-1}(\tau)[A(\tau)F(\tau) - F'(\tau)]\tilde{\eta}(\tau) + \\ F^{-1}(\tau)B(\tau)\bar{u}(\tau)\end{aligned}\quad (72)$$

To produce n uncoupled differential equations before control is applied, the term

$$F^{-1}(\tau)[A(\tau)F(\tau) - F'(\tau)]$$

must be diagonal. Recalling Equation (59), Floquet theory provides the result,

$$F'(\tau) = A(\tau)F(\tau) - F(\tau)J$$

or by rearranging,

$$J = F^{-1}(\tau)[A(\tau)F(\tau) - F'(\tau)]\quad (73)$$

Thus, by substituting this result of Floquet theory into Equation (72) the uncontrolled decoupled modal differential equations are found,

$$\dot{\tilde{\eta}}'(\tau) = J\tilde{\eta}(\tau) + F^{-1}(\tau)B(\tau)\bar{u}(\tau)\quad (74)$$

where J , from Chapter III, is a Jordan form matrix composed of the n characteristic exponents.

Mode-Controllability Matrix

The mode-controllability matrix of Equation (74) consists of two elements: the $F^{-1}(\tau)$ and the $B(\tau)$ matrices. Defined as the product,

$$R(\tau) = F^{-1}(\tau)B(\tau) \quad (75)$$

the mode-controllability matrix identifies the modes of the system that are controllable (Ref. 13: 67). The matrix $B(\tau)$ identifies the physical coordinates to which control is applied. As such, it is, to some extent, available as an option to the control engineer. However, the control must be applied to the system in a scheme that is physically realizable.

When the attitude of a satellite is being controlled, the control is applied to the angular velocity of the body about the three axes. Generally, this control is applied via gas jets or small thrusters. For the satellite cases discussed in Chapter II, a suitable $B(\tau)$ matrix to accomplish this control, with a scalar control law, is:

$$B(\tau)=B=\begin{bmatrix} 0 \\ 0 \\ 1 \\ 1 \end{bmatrix} \quad (76)$$

Thus, as the control is applied, the angular velocity of θ_1 and θ_2 change, resulting in a corresponding change in angular displacement.

The remaining component of the mode-controllability matrix is $F^{-1}(\tau)$, which from Chapter III is a periodic matrix. This matrix may be found by integrating Equation (59) to obtain $F(\tau)$ and then inverting the result. Since

$F(\tau)$ must be inverted at every instance control is applied, this would require extensive computation time or $F^{-1}(\tau)$ may be calculated directly by noting:

$$F^{-1}(\tau)F(\tau) = [I]$$

Differentiating this with respect to τ ,

$$F^{-1}{}'(\tau)F(\tau) + F^{-1}(\tau)F'(\tau) = 0$$

Substituting Equation (59) into this result,

$$F^{-1}{}'(\tau) = F^{-1}(\tau)[F(\tau)J - A(\tau)F(\tau)]F^{-1}(\tau)$$

and finally, by simplifying,

$$F^{-1}{}'(\tau) = JF^{-1}(\tau) - F^{-1}(\tau)A(\tau) \quad (77)$$

Integrating this matrix differential with the initial condition $F^{-1}(0)$ over one period finds $F^{-1}(\tau)$ for all τ . With $F^{-1}(\tau)$ and B , the mode-controllability matrix, is defined, which since $F^{-1}(\tau)$ is periodic, is periodic. Finally, by defining the control law $\bar{u}(\tau)$, the periodic system can be controlled and further evaluations made.

Control Law

Since the purpose of this controller is to stabilize the attitude motion, the controller attempts to drive the states to zero. To regulate this system, a feedback control law consisting of a gain matrix, K , times the modal vector is used:

$$\bar{u} = K\bar{\eta}(\tau) \quad (78)$$

where

$$K = [k_1 \ k_2 \ k_3 \ k_4]$$

Since K is a row matrix, the control vector reduces to a scalar control law of the form

$$u = k_1 \eta_1(\tau) + k_2 \eta_2(\tau) + k_3 \eta_3(\tau) + k_4 \eta_4(\tau) \quad (79)$$

With this control law, the general form of the closed-loop system is:

$$\begin{aligned} \bar{\eta}'(\tau) = & \begin{bmatrix} \lambda_1 & 0 & 0 & 0 \\ 0 & \lambda_2 & 0 & 0 \\ 0 & 0 & \lambda_3 & 0 \\ 0 & 0 & 0 & \lambda_4 \end{bmatrix} \bar{\eta}(\tau) + \\ & \begin{bmatrix} R_1 k_1 & R_1 k_2 & R_1 k_3 & R_1 k_4 \\ R_2 k_1 & R_2 k_2 & R_2 k_3 & R_2 k_4 \\ R_3 k_1 & R_3 k_2 & R_3 k_3 & R_3 k_4 \\ R_4 k_1 & R_4 k_2 & R_4 k_3 & R_4 k_4 \end{bmatrix} \bar{\eta}(\tau) \end{aligned} \quad (80)$$

or, by simplification

$$\bar{\eta}'(\tau) = \begin{bmatrix} \lambda_1 + R_1 k_1 & R_1 k_2 & R_1 k_3 & R_1 k_4 \\ R_2 k_1 & \lambda_2 + R_2 k_2 & R_2 k_3 & R_2 k_4 \\ R_3 k_1 & R_3 k_2 & \lambda_3 + R_3 k_3 & R_3 k_4 \\ R_4 k_1 & R_4 k_2 & R_4 k_3 & \lambda_4 + R_4 k_4 \end{bmatrix} \bar{\eta}(\tau) \quad (81a)$$

which is in the form,

$$\bar{\eta}'(\tau) = A^*(\tau)\bar{\eta}(\tau) \quad (81b)$$

where R_i indicates the i^{th} component of the mode-controllability matrix. Recalling from the discussion of the mode-controllability matrix that $R(\tau)$ is periodic, the closed-loop system given by Equations (81) is also periodic in the form of Equation (43). As such, the asymptotic stability of this closed-loop system can be established using Floquet theory. Thus, the performance of this controller can be readily evaluated by finding the eigenvalues of the closed-loop monodromy matrix.

Control Law Implementation

Using the control law given by Equation (78), any mode or number of modes can be controlled. Control of a mode is accomplished by having a non-zero gain in the K matrix at a position corresponding to the mode requiring control. Thus, if the second and fourth modes requires control, that is, $\eta_2(\tau)$ and $\eta_4(\tau)$ have undesirable characteristics, the gain matrix is

$$K = \begin{bmatrix} 0 & k_2 & 0 & k_4 \end{bmatrix} \quad (82)$$

This would produce the closed-loop system as follows:

$$\dot{\bar{\eta}}'(\tau) = \begin{bmatrix} \lambda_1 & R_1 k_2 & 0 & R_1 k_4 \\ 0 & \lambda_2 + R_2 k_2 & 0 & R_2 k_4 \\ 0 & R_3 k_2 & \lambda_3 & R_3 k_4 \\ 0 & R_4 k_2 & 0 & \lambda_4 + R_4 k_4 \end{bmatrix} \bar{\eta}(\tau) \quad (85)$$

By inspection, the characteristic exponents of this system

are λ_1 and λ_3 , which remained unchanged, and the controlled characteristic exponents, λ_2^* and λ_4^* . Examining Equations (80) and (81), as the control is applied to the system, the n uncoupled differential equations are coupled by the additional elements in the columns of the Jordan form matrix corresponding to the controlled modes. Two general cases appear when control is applied. The first case occurs when there is one controlled mode, and the other is when there are multiple controlled modes.

Single Controlled Mode. When only one mode is controlled, the closed-loop system can always be rearranged so that the coefficient matrix is in either upper or lower triangular form. In triangular form, the differential equation for the controlled mode can be solved. With this solution, the stability can be determined directly. In fact, the location of the controlled characteristic exponent is a linear function of its uncontrolled location, the appropriate element of the mode-controllability matrix, and the gain. All of these features are demonstrated in the following example.

Suppose the original system had a unstable mode corresponding to $\tau_3(\tau)$. Using Equations (78) and (79), the control law is

$$u = k_3 \eta_3(\tau) \quad (84)$$

and the closed-loop system (from Equation (81a)) is,

$$\bar{\eta}'(\tau) = \begin{bmatrix} \lambda_1 & 0 & R_1 k_3 & 0 \\ 0 & \lambda_2 & R_2 k_3 & 0 \\ 0 & 0 & \lambda_3 + R_3 k_3 & 0 \\ 0 & 0 & R_4 k_3 & \lambda_4 \end{bmatrix} \bar{\eta}(\tau) \quad (85)$$

Rearranging this set of differential equations,

$$\begin{bmatrix} \eta_1'(\tau) \\ \eta_2'(\tau) \\ \eta_4'(\tau) \\ \eta_3'(\tau) \end{bmatrix} = \begin{bmatrix} \lambda_1 & 0 & 0 & R_1 k_3 \\ 0 & \lambda_2 & 0 & R_2 k_3 \\ 0 & 0 & \lambda_4 & R_4 k_3 \\ 0 & 0 & 0 & \lambda_3 + R_3 k_3 \end{bmatrix} \begin{bmatrix} \eta_1(\tau) \\ \eta_2(\tau) \\ \eta_4(\tau) \\ \eta_3(\tau) \end{bmatrix} \quad (86)$$

where the coefficient matrix is in upper triangular form.

As such, the solution for $\eta_3(\tau)$ is found using an integrating factor. From Equation (85), the differential equation for $\eta_3(\tau)$ is

$$\eta_3'(\tau) - [\lambda_3 + R_3(\tau)k_3] \eta_3(\tau) = 0 \quad (87)$$

which is a linear homogeneous first order differential equation. Using an integrating factor of the form

$$\eta_3(\tau) = \exp\left\{-\int_0^\tau [\lambda_3 + R_3(\xi)k_3] d\xi\right\}$$

an exact differential for $\eta_3(\tau)$ can be found (Ref. 10: 24).

Multiplying Equation (87) by this integrating factor

$$\begin{aligned} \eta_3'(\tau) \exp\left\{-\int_0^\tau [\lambda_3 + R_3(\xi)k_3] d\xi\right\} - \exp\left\{-\int_0^\tau [\lambda_3 + R_3(\xi)k_3] d\xi\right\} [\lambda_3 + R_3(\tau)k_3] \eta_3(\tau) &= 0 \end{aligned} \quad (88)$$

which, by inspection, is the exact differential

$$\frac{d}{d\tau} [\eta_3(\tau) \exp\{-\int_0^\tau [\lambda_3 + R_3(\xi)k_3] d\xi\}] = 0 \quad (89)$$

Since Equation (89) is an exact differential,

$$\eta_3(\tau) \exp\{-\int_0^\tau [\lambda_3 + R_3(\xi)k_3] d\xi\} = C \quad (90)$$

where C is the constant of integration. This constant can be found by setting τ equal to zero:

$$\begin{aligned} \eta_3(0) \exp(0) &= C \\ \eta_3(0) &= \eta_{30} \end{aligned}$$

Rearranging Equation (90), the solution for the controlled mode is found,

$$\eta_3(\tau) = \eta_{30} \exp\left\{\int_0^\tau [\lambda_3 + R_3(\xi)k_3] d\xi\right\} \quad (91)$$

Recalling that the mode-controllability matrix is periodic, Equation (91) can be simplified further by representing $R_3(\xi)$ as an infinite Fourier series (Ref. 10: 387):

$$\begin{aligned} R_3(\xi) &= a_0 + \sum_{n=1}^{\infty} a_n \cos \frac{2n\pi}{T} \xi + \\ &\quad + \sum_{n=1}^{\infty} b_n \sin \frac{2n\pi}{T} \xi \end{aligned} \quad (92)$$

where the coefficients are given by the Euler formulas:

$$\begin{aligned} a_0 &= \frac{1}{T} \int_0^T R_3(\xi) d\xi \\ a_n &= \frac{1}{T} \int_0^T R_3(\xi) \cos \frac{2n\pi}{T} \xi d\xi \quad (\xi \in (-T/2, T/2)) \end{aligned}$$

and

$$b_n = \frac{1}{T} \int_0^T R_3(\xi) \sin \frac{2n\pi}{T} \xi d\xi$$

Substituting Equation (92) into Equation (91) one obtains

$$\eta_3(\tau) = \eta_{3_0} \exp[(\lambda_3 + a_0 k_3)\tau] \exp\left\{\int_0^\tau R_{3p}(\xi) k_3 d\xi\right\} \quad (93)$$

where R_{3p} represents the periodic portion of R_3 . Since the asymptotic stability of the closed-loop system depends on the eigenvalues, or characteristic multiples, of the monodromy matrix of Equation (87), the eigenvalue associated with the controlled mode is given by Equation (93) evaluated at $\tau = T$, with $\eta_{3_0} = 1$. Evaluating Equation (93),

$$\eta_3(T) = \exp[(\lambda_3 + a_0 k_3)T] \exp\left\{\int_0^T R_{3p}(\xi) k_3 d\xi\right\} \quad (94)$$

where

$$\int_0^T R_{3p}(\xi) k_3 d\xi = 0$$

Simplifying this result,

$$\eta_3(T) = \exp[(\lambda_3 + a_0 k_3)T] \quad (95)$$

or, the controlled system characteristic exponent is given by Equation (54)

$$\lambda_3^* = \frac{\ln}{T} \exp[(\lambda_3 + a_0 k_3)T] = \lambda_3 + a_0 k_3 \quad (96)$$

Thus, the closed-loop characteristic exponent is found by this linear equation, and with the gain value such that

$$\lambda_3 + a_0 k_3 < 0$$

stability is assured.

From Equation (97), control of a single mode is predicated on the constant, i.e. zero frequency, portion of $R_3(\tau)$ being non-zero. If the constant portion is equal to zero, stability can still be achieved by allowing the gain to be periodic of the form,

$$k_3(\tau) = k_3 \cos \frac{2\pi\tau i}{T} \quad (98a)$$

or

$$k_3(\tau) = k_3 \sin \frac{2\pi\tau i}{T} \quad (98b)$$

where i is the index of some non-zero Fourier coefficient of $R(\tau)$. Using this non-constant gain along with the trigonometric identities,

$$\sin^2\tau = \frac{1}{2}(1 - \cos 2\tau) \quad (99a)$$

$$\cos^2\tau = \frac{1}{2}(1 + \cos 2\tau) \quad (99b)$$

a non-zero constant portion of $R_3(\tau)$ is generated. This procedure is demonstrated as follows, using Equation (98a),

$$k_3(\tau) = k_3 \cos \frac{2\pi\tau}{T} j$$

Multiplying this result by the appropriate element of the mode-controllability matrix, one finds,

$$\begin{aligned} R_3(\tau)k_3(\tau) &= a_0 k_3 \cos \frac{2\pi\tau}{T} j + \sum_{\substack{i=1 \\ i \neq j}}^{\infty} (a_i \cos \frac{2\pi\tau}{T} i) \\ &+ (k_3 \cos \frac{2\pi\tau}{T} j) + \sum_{i=1}^{\infty} (b_i \sin \frac{2\pi\tau}{T} i) (k_3 \cos \frac{2\pi\tau}{T} j) \\ &+ a_j k_3 \cos^2 \frac{2\pi\tau}{T} j \end{aligned} \quad (100)$$

With the last term of this result and Equation (99b), a constant portion is generated:

$$a_j k_3 \cos^2 \frac{2\pi\tau}{T} j = \frac{a_j k_3}{2} (1 + \cos \frac{4\pi\tau}{T} j)$$

or the constant portion is

$$a'_c = \frac{a_j}{2}$$

With the result, the controlled mode is always controllable provided $R_3(\tau)$ is not zero for all τ . Otherwise, if $R_3(\tau) = 0$, the third mode is uncontrollable. This is the result that the mode-controllability matrix indicates.

Thus, when there is one controlled mode, the solution to the closed-loop periodic differential equation can be solved using an integrating factor. Using this result, the stability of the closed-loop controlled mode can be determined directly by using Equation (96). Since modal control only controls the desired mode(s), the stability of the other modes is unaffected by the control, and the stability of the entire system is assured.

Multiple Controlled Modes. When there are multiple controlled modes, the stability is not as readily attainable as it was in the previous case. The reason for this is that the closed-loop coefficient matrix can not be rearranged to form a triangular form, either upper or lower, matrix. Since the matrix is not in triangular form, the solution to the differential equations for the controlled modes are not readily

obtained. As an example, suppose the original system had two unstable modes, $\eta_2(\tau)$ and $\eta_3(\tau)$. From Equation (81a), the closed-loop system is represented by

$$\bar{\eta}'(\tau) = \begin{bmatrix} \lambda_1 & R_{12} k_2 & R_{13} k_3 & 0 \\ 0 & \lambda_2 + R_{22} k_2 & R_{23} k_3 & 0 \\ 0 & R_{32} k_2 & \lambda_3 + R_{33} k_3 & 0 \\ 0 & R_{42} k_2 & R_{43} k_3 & \lambda_4 \end{bmatrix} \bar{\eta}(\tau) \quad (102)$$

Unlike the case when only one mode is controlled, the coefficient matrix of this equation can not be rearranged into a triangular form. Therefore, to find the closed-loop characteristic exponents a Floquet theory analysis using the concepts presented in Chapter III must be completed.

By inspection of Equation (102), the closed-loop characteristic exponent are λ_1 , λ_4 and the two found from the monodromy matrix calculated by integrating the sub-matrix,

$$\psi'(\tau) = \begin{bmatrix} R_{22} k_2 + \lambda_2 & R_{23} k_3 \\ R_{32} k_2 & \lambda_3 + R_{33} k_3 \end{bmatrix} \phi(\tau)$$

There are essentially two methods of setting the gains to stabilize this system. The first method consists of a systematic search using various gain settings until the desired characteristic exponents are found. The second method entails successive diagonalization. In this method, one gain is set resulting in a controlled system. Then

this controlled system is re-diagonalized to form a new Jordan form matrix and another gain is then set. This process is repeated until all modes are stabilized.

This completes the development of the control law and the mode-controllability matrix. This control law presented in this chapter is capable of controlling any number of modes. In the following chapter, example test cases from both the symmetric and unsymmetric satellites are used to demonstrate the actual usage of this control law.

CHAPTER V

RESULTS

In Chapter II of this study, the development of linearized equations for the attitude motion of two satellites was presented. In both cases, the stability of these periodic systems was found to be dependent on various parameters, including the orbital eccentricity, moment of inertia ratios, and spin rates. Obviously, by varying these parameters, an infinite number of test cases are found. Therefore, five example test cases were selected from these two satellite cases. Using these five test cases, the theoretical developments of this study are verified with numerical results. Upon selecting the five test cases, a stability analysis, using Floquet theory and the results of Chapter III, is conducted. With this stability analysis, two of the test cases are digitally simulated to verify the results. Next, three of the test cases are controlled using the developments of Chapter IV and the closed-loop linear system is simulated. Finally, numerical problems which appeared several times are presented using one of the test cases.

Test Cases

From the infinite number of combinations of satellite parameters, five test cases are chosen for use during

the presentation of the numerical results. Of these five, two are symmetrical satellites in elliptical orbits, and the remaining three are unsymmetrical satellites in circular orbits. Table III is a summary of these five test cases and their associated parametric values. The test cases numbers are used throughout this chapter to identify the individual cases.

Table III
Parametric Values of the Five Test Cases

Test Case	e	α	k_1	k_2
1	0.5	-1.0	1.0	---
2	0.5	-2.0	.6	---
3	0.0	-1.0	.2	-.6
4	0.0	1.0	-.6	.6
5	0.0	1.0	-1.0	-.3

Stability Analysis

The first step in the control of an arbitrary satellite design is to conduct a stability analysis of the open loop system. When the linear system has constant coefficients, the stability is easily determined by the eigenvalues of the coefficient matrix. However, when the system is periodic, Floquet theory is used to ascertain the asymptotic stability. Using the theory of Chapter III, the stability

of the five satellite cases is determined. Table IV contains the four characteristic exponents found using Floquet theory for each test case. From Chapter III, asymptotic stability is assured if the real part of all characteristic exponents is less than zero.

Table IV
Characteristic Exponents of the Five Test Cases

Case	λ_1	λ_2	λ_3	λ_4
1	.6718	-.6718	0.0 +.5728i	0.0 -.3728i
2	0.0 +.1206i	0.0 -.1206i	0.0 +.4005i	0.0 -.4005i
3	.1258	-.1258	0.0 +.1819i	0.0 -.1819i
4	.3557 +.1776i	.3557 -.1776i	-.3557 +.1776i	-.3557 -.1776i
5	.8265	-.8265	.2128	.2128

When the characteristic exponents have a real part of zero, the system exhibits neutral stability. Of the five test cases, all are unstable except Case 2. Case 2 is stable, and it exhibits the characteristics of stable gravity gradient satellites mentioned in Chapter I. With the characteristic exponents for Case 2, a stable satellite has zero damping and low natural frequencies of oscillation. Thus, the four modes of this stable case are pure oscillatory: very undesirable

attitude motion for a precise satellite system. Cases 1 and 3 have one unstable mode, and Cases 4 and 5 have two unstable modes. Cases 1 and 3 both have one unstable real characteristic exponent, Case 4 has two unstable complex conjugate characteristic exponents, and Case 5 has two unstable real characteristic exponents.

To validate the results of the stability analysis, the uncontrolled linear systems of Cases 2 and 3 were simulated over fifteen periods. At first, the uncontrolled system of Case 2 was simulated using physical coordinates as the basis variables. The results are presented in Figures 2 through 5. As expected, no specific trends on asymptotic stability are ascertained from these figures. The reason for the simulation results appearing as they do is that the state variables are actually linear combinations of the four modes. The characteristic exponents represent the response of the individual modes, not the physical state variables. From Equation (71),

$$\tilde{\mathbf{x}}(\tau) = \mathbf{P}(\tau)\tilde{\mathbf{q}}(\tau)$$

and the state variable responses are linear combinations of the responses of the individual modes. Therefore, to gain more insight into the responses of the various test cases when simulated, all simulation results are presented in modal variables.

The initial conditions used throughout this study, for simulation purposes are:

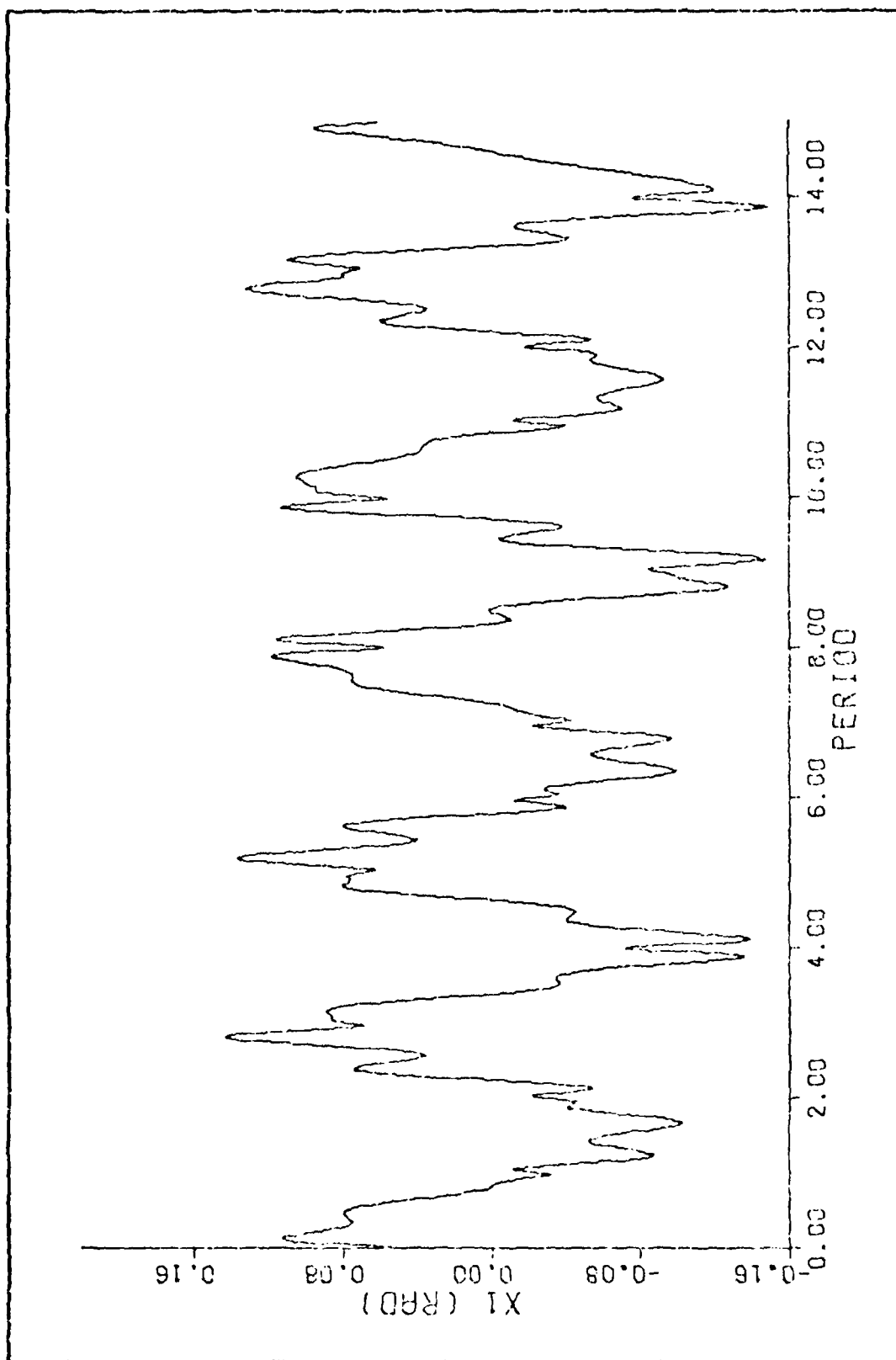


Figure 2. Uncontrolled $x_1(\tau)$ Response for Case 2

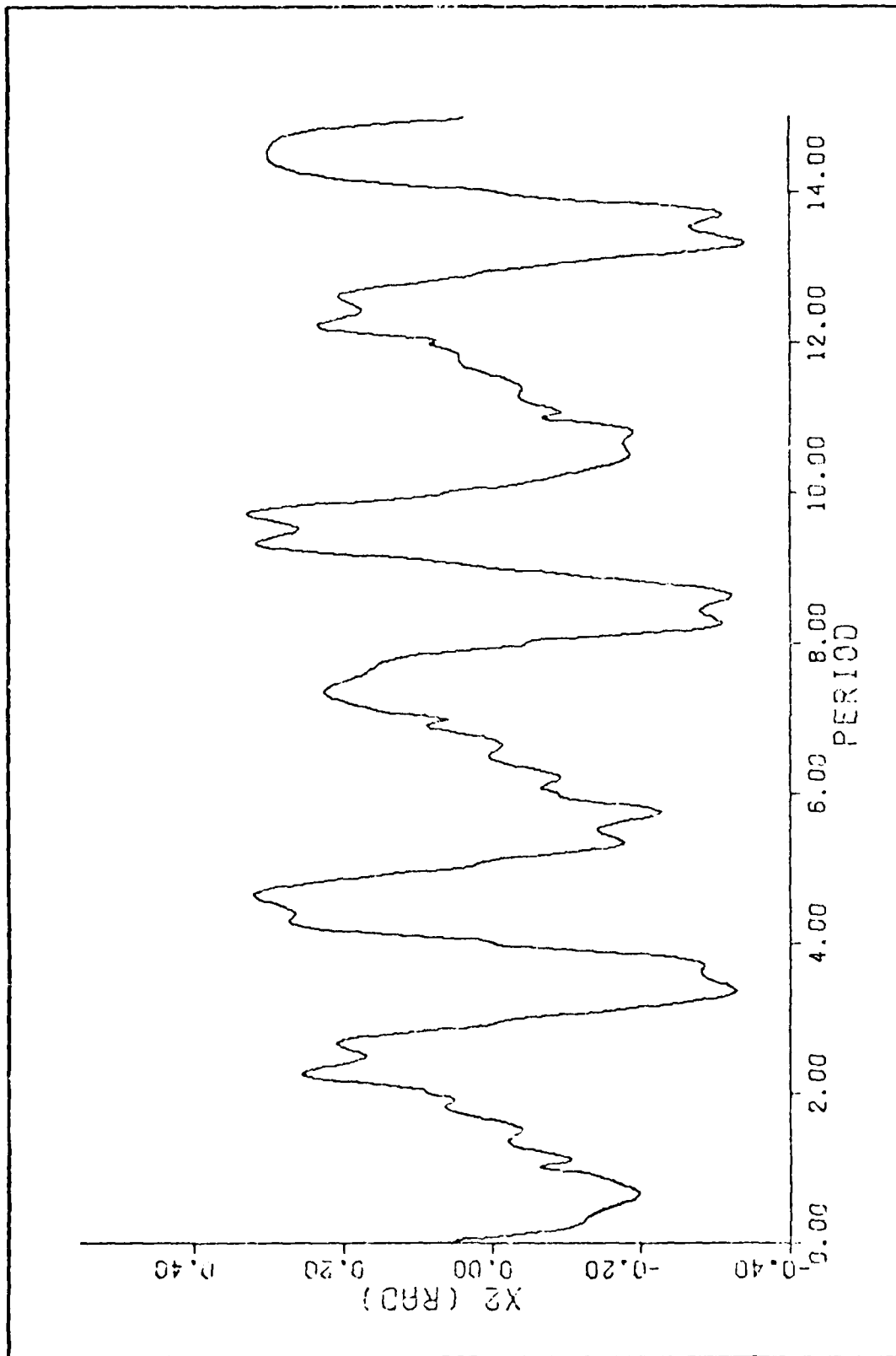


Figure 3. Uncontrolled $x_2(\tau)$ Response for Case 2

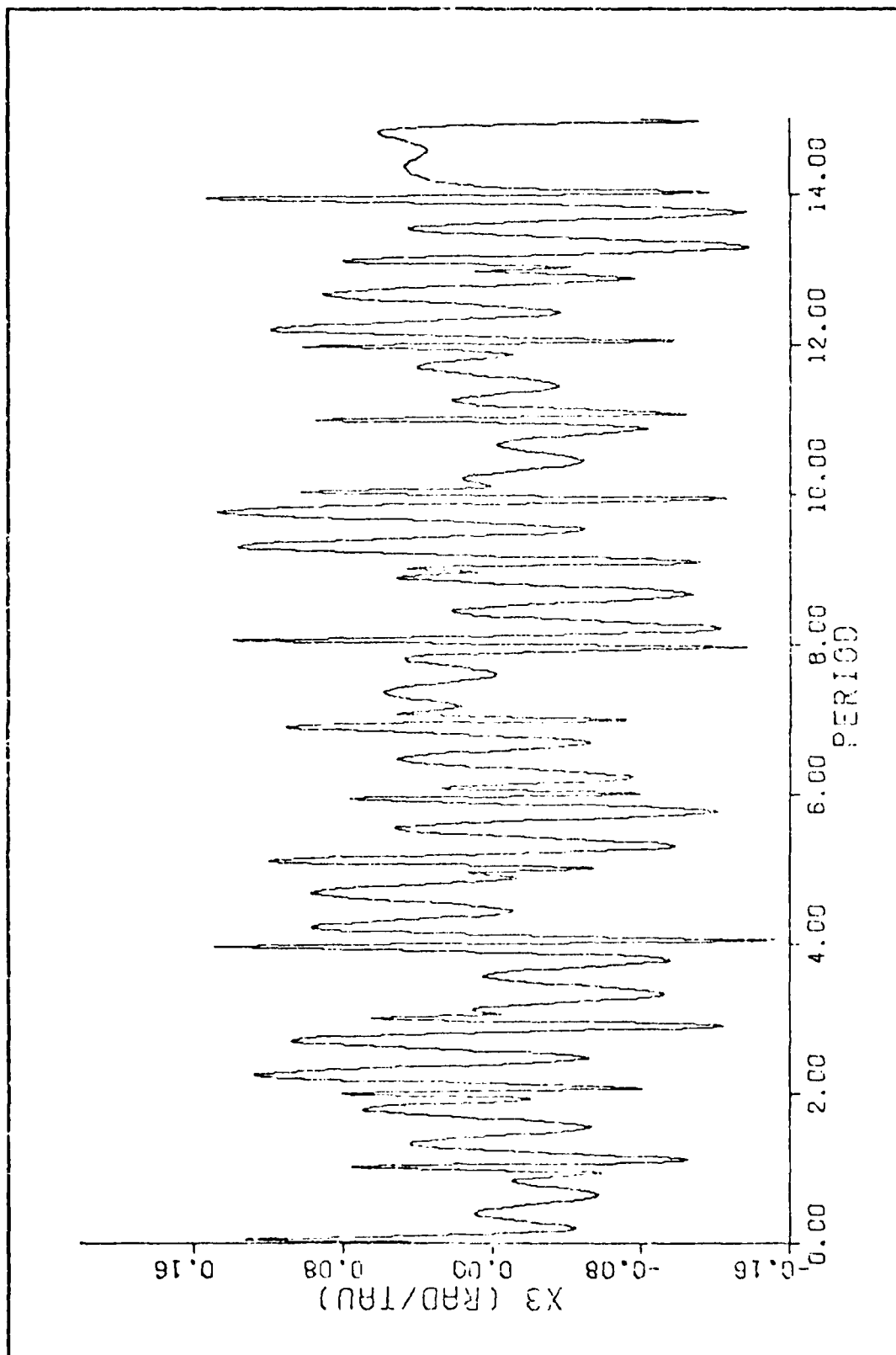


Figure 4. Uncontrolled $x_3(\tau)$ Response for Case 2

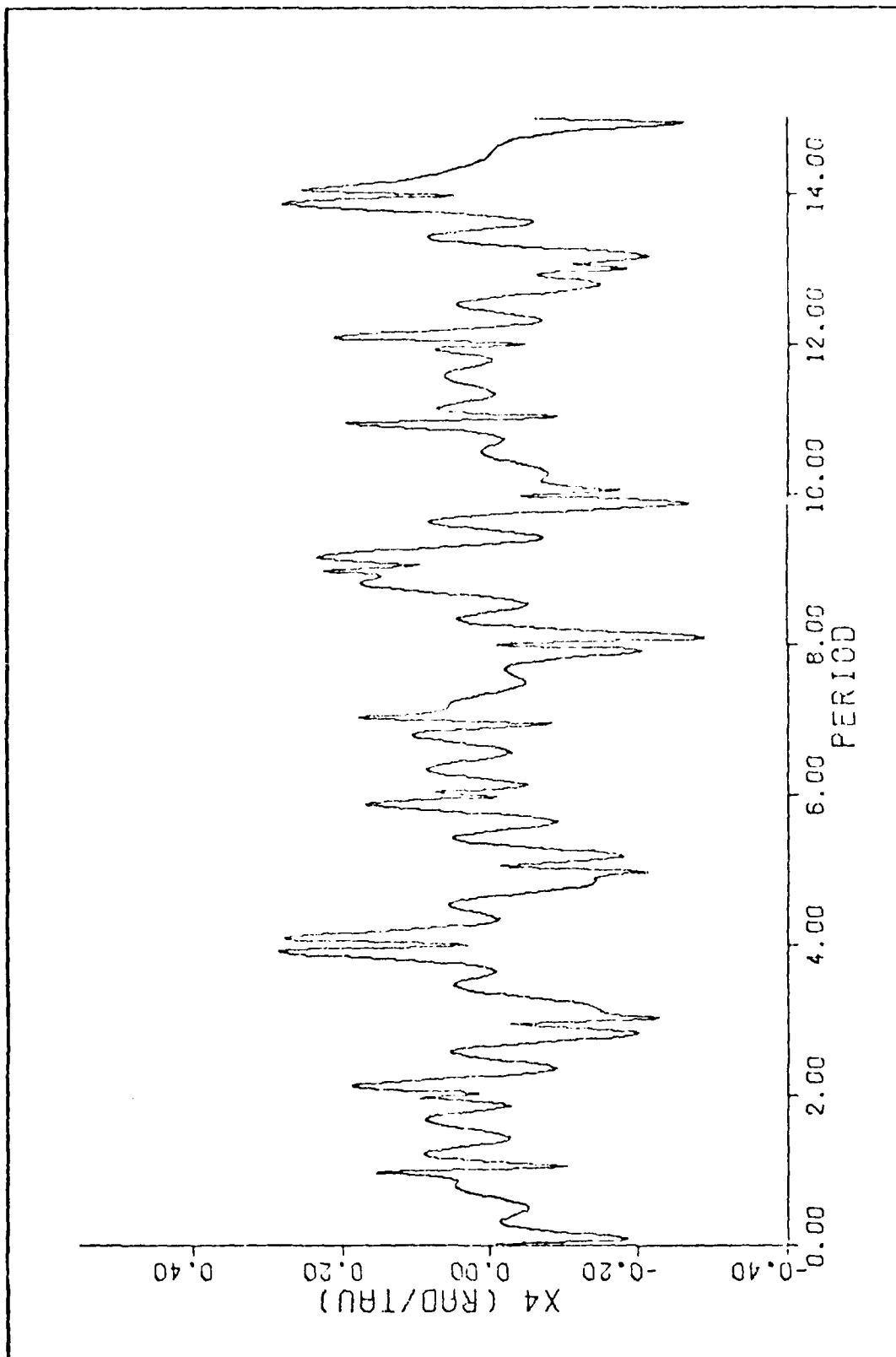


Figure 5. Uncontrolled $x_u(\tau)$ Response for Case 2

$$\bar{x}(0) = \begin{bmatrix} .3 \\ .3 \\ .3 \\ .3 \end{bmatrix}$$

This initial conditions vector was chosen to assure that all modes are excited. Also, all simulation results are over a total of fifteen periods. This period length was assumed to be of sufficient length to illustrate the general trends in stability of the linearized equations.

Simulating Case 2 in modal coordinates, a response typical of a stable gravity gradient satellite is obtained. The responses of the individual modes to the input initial conditions are presented in Figures 6 through 9. As expected, the first and second modes represent the extremely low frequency oscillations and the third and fourth modes represent the slightly higher frequency oscillations. Also, from Figures 8 and 9, no damping of the oscillatory motion is observed.

To verify the instability caused by positive real parts of the characteristic exponents, Case 3 was simulated. From Table IV, the first mode is unstable. Figures 10 through 13 depict the responses of the four modes of Case 3. As expected, the first mode, the mode with positive real characteristic exponent, is definitely unstable. The stable real mode, the second mode, demonstrates the typical response for a mode with a negative real portion. Finally, the third

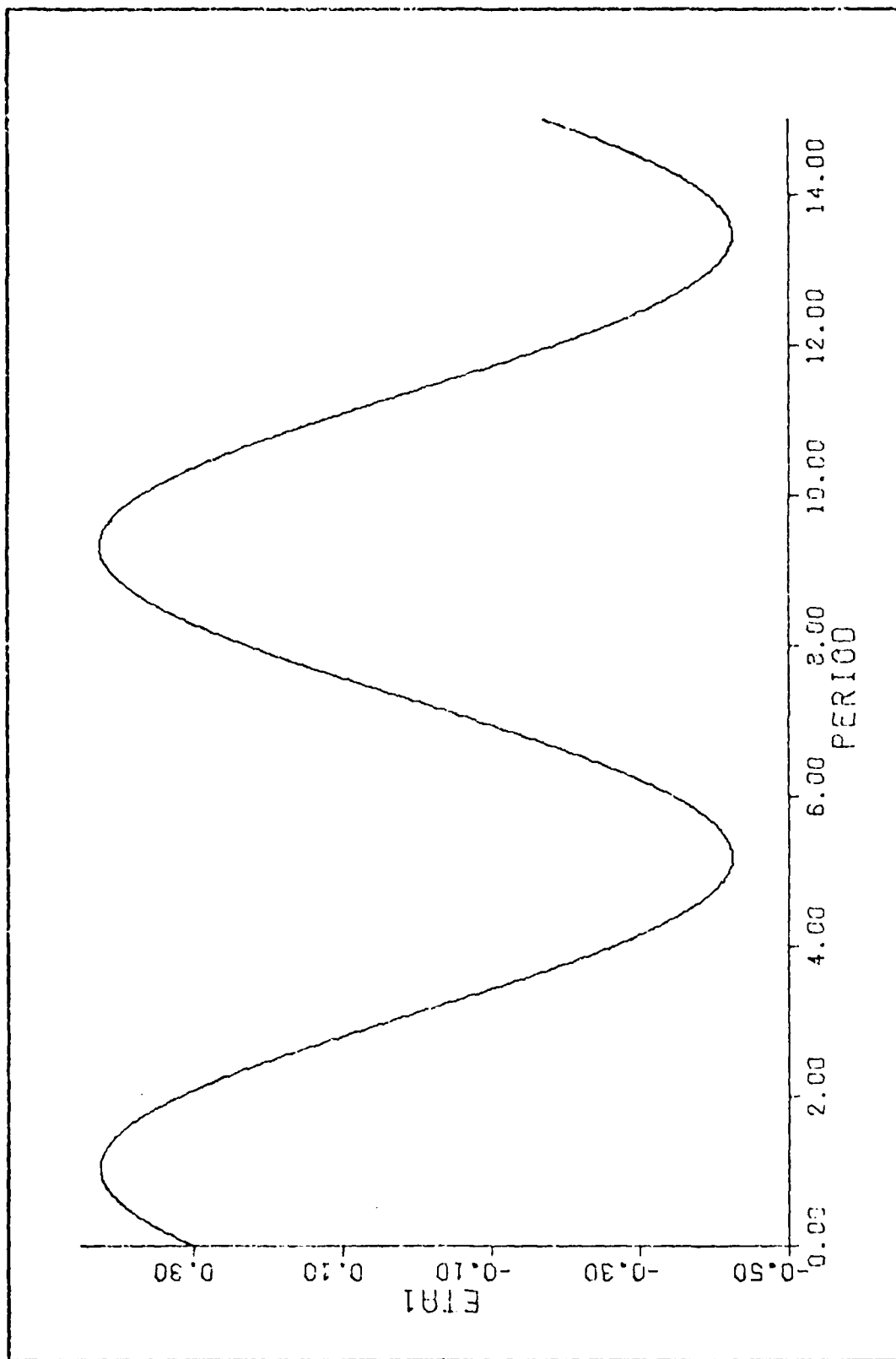


Figure 6. Uncontrolled First Mode Response for Case 2

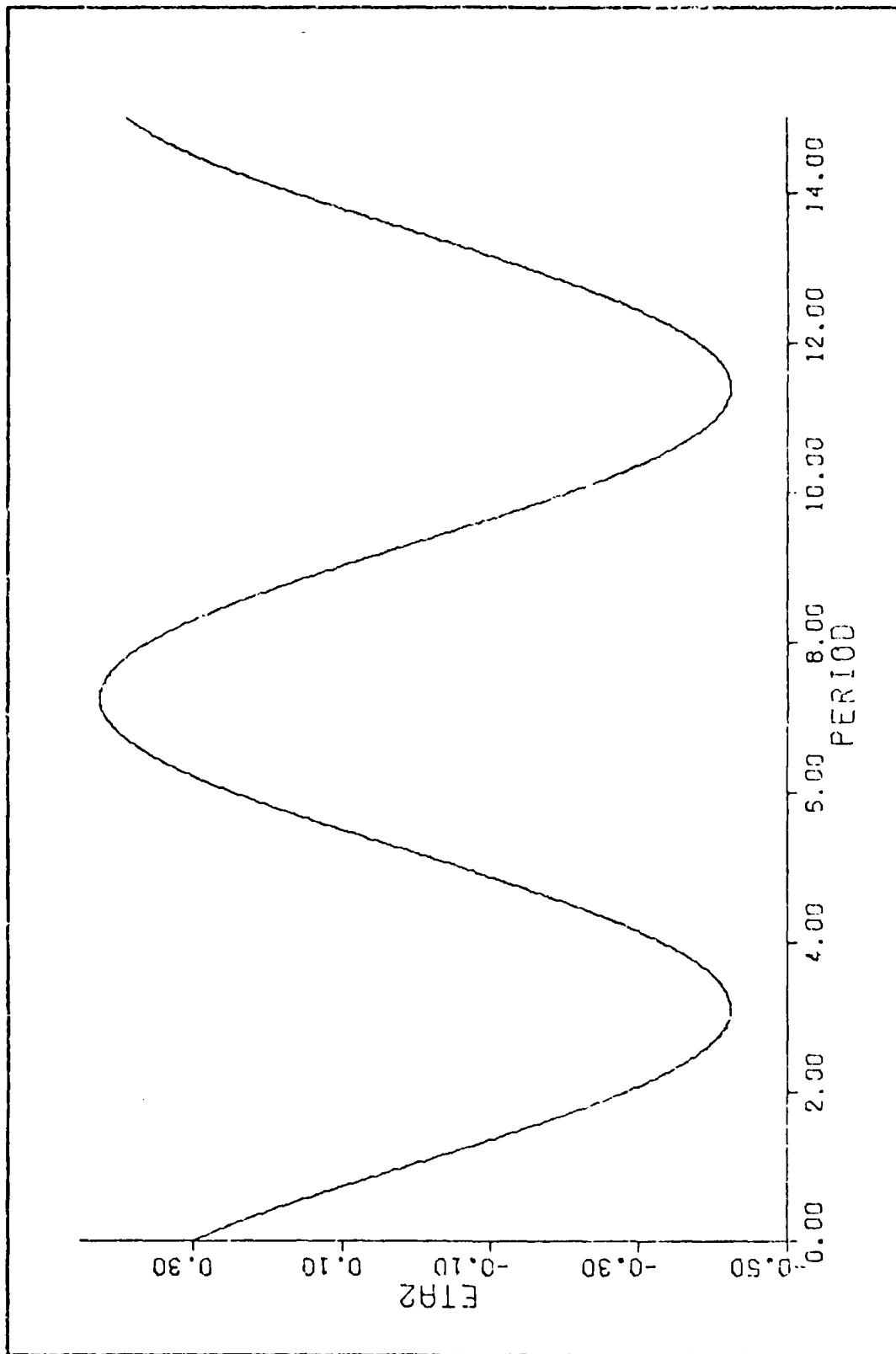


Figure 7. Uncontrolled Second Mode Response for Case 2

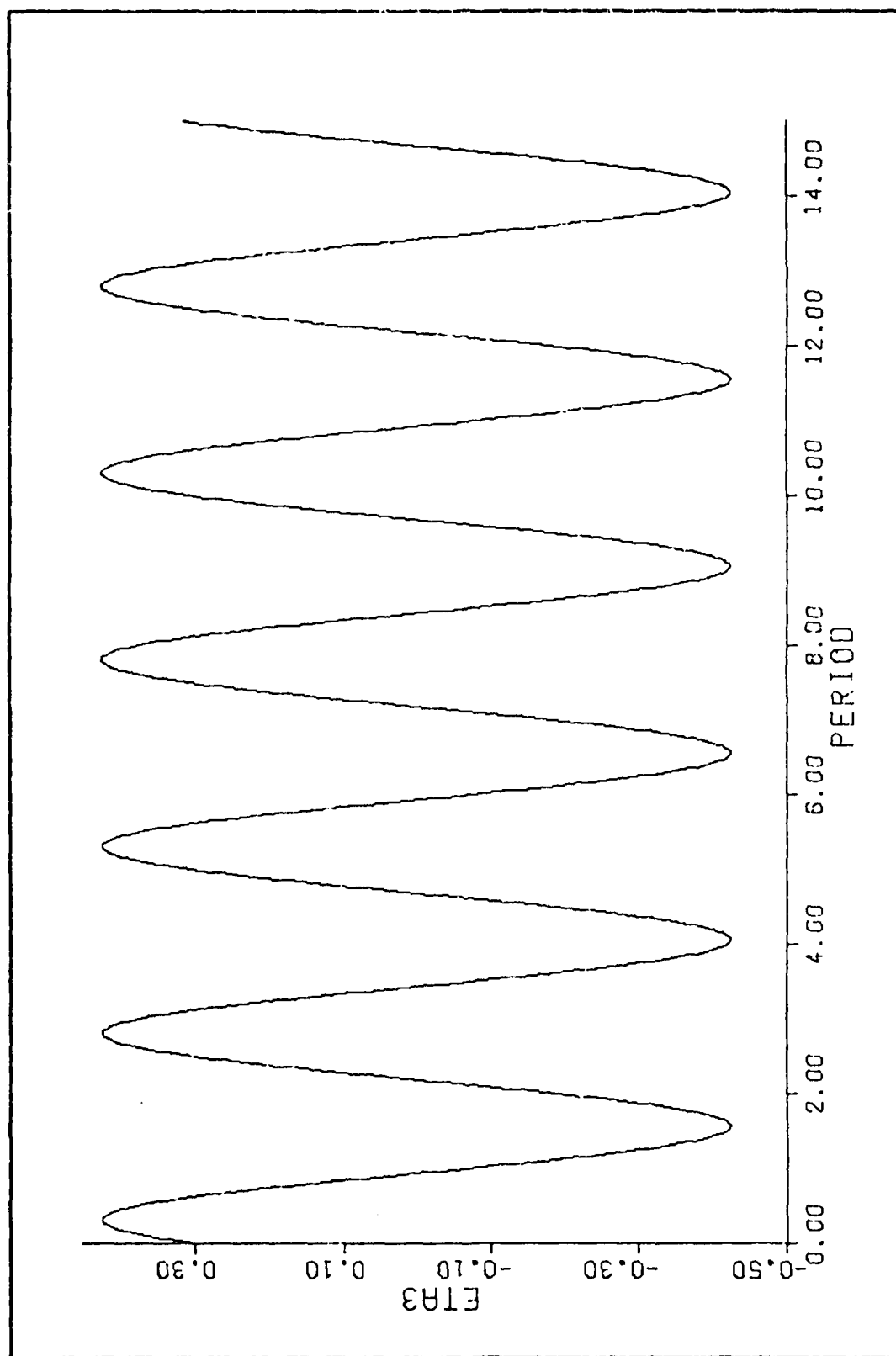


Figure 8. Uncontrolled Third Mode Response for Case 2

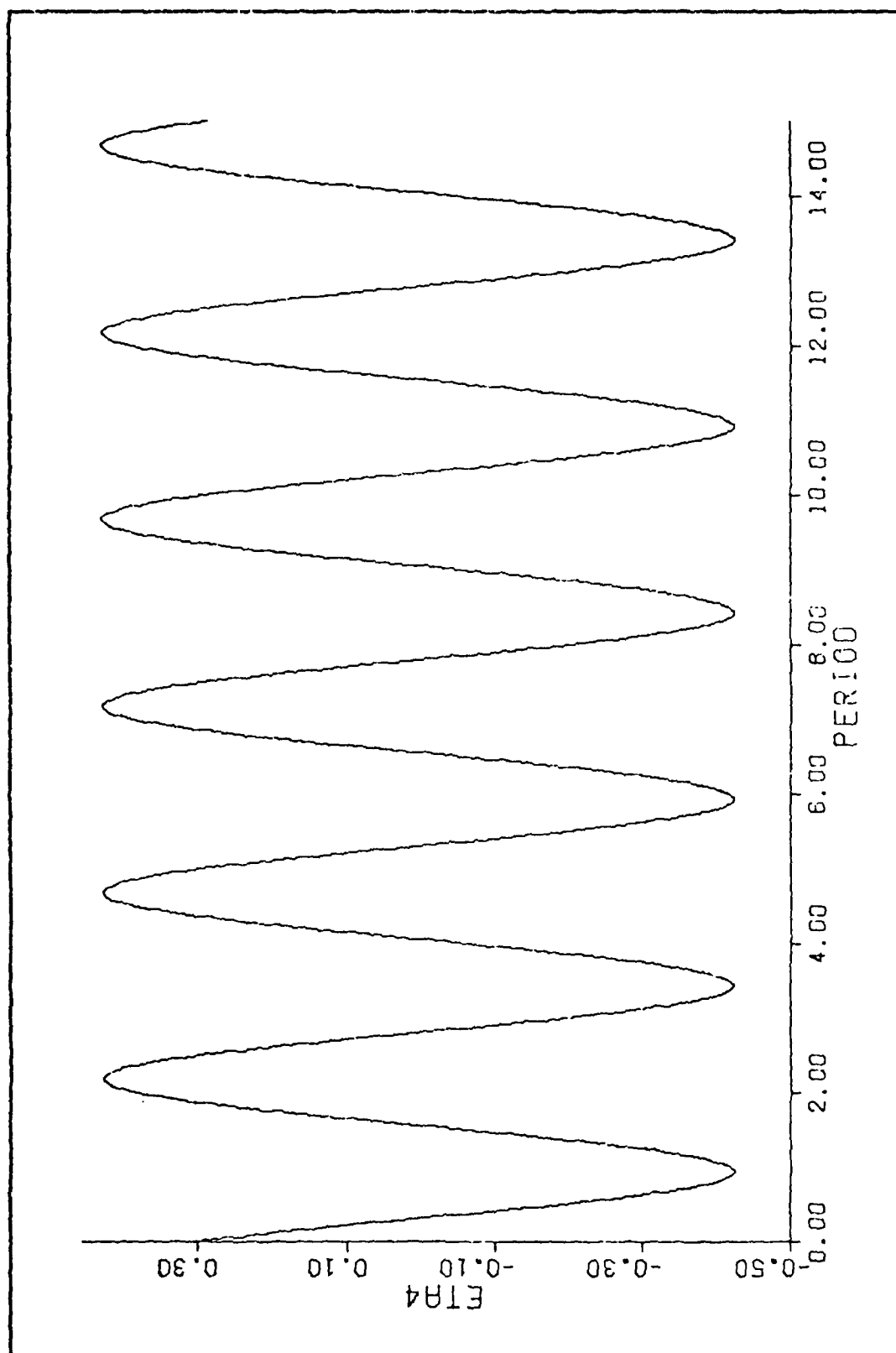


Figure 9. Uncontrolled Fourth Mode Response for Case 2

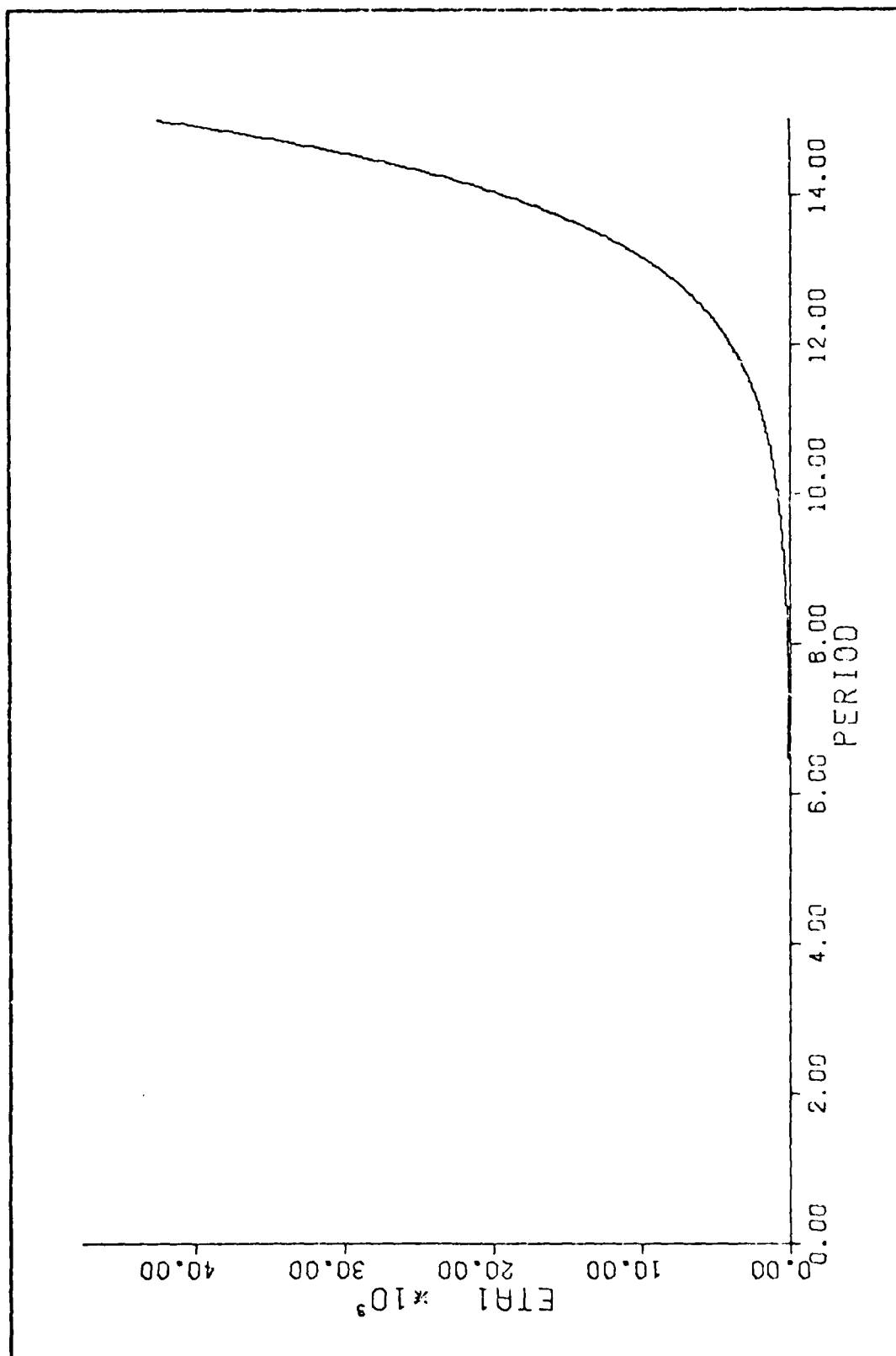


Figure 10. Uncontrolled First Mode Response for Case 3

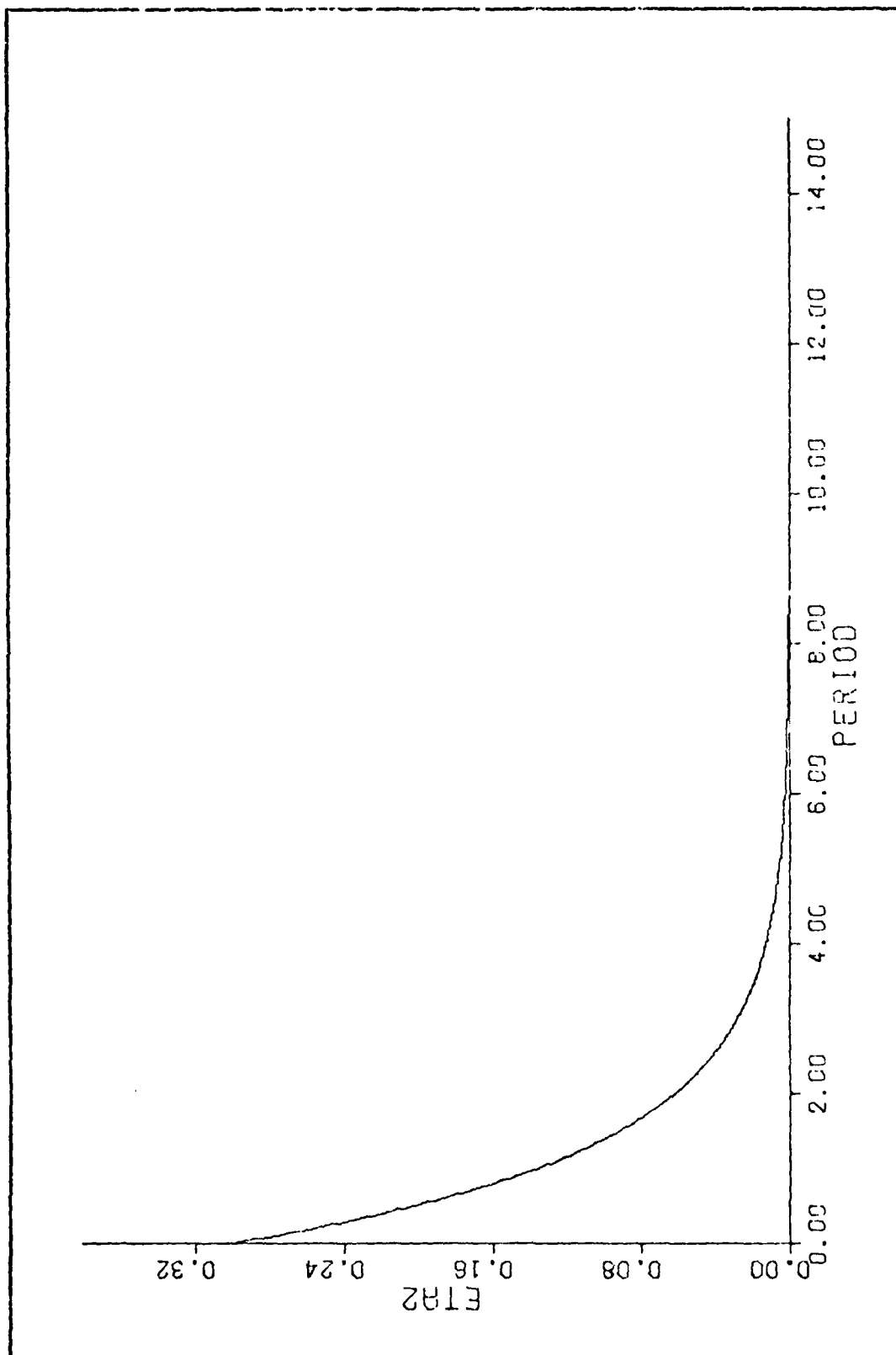


Figure 11. Uncontrolled Second Mode Response for Case 3

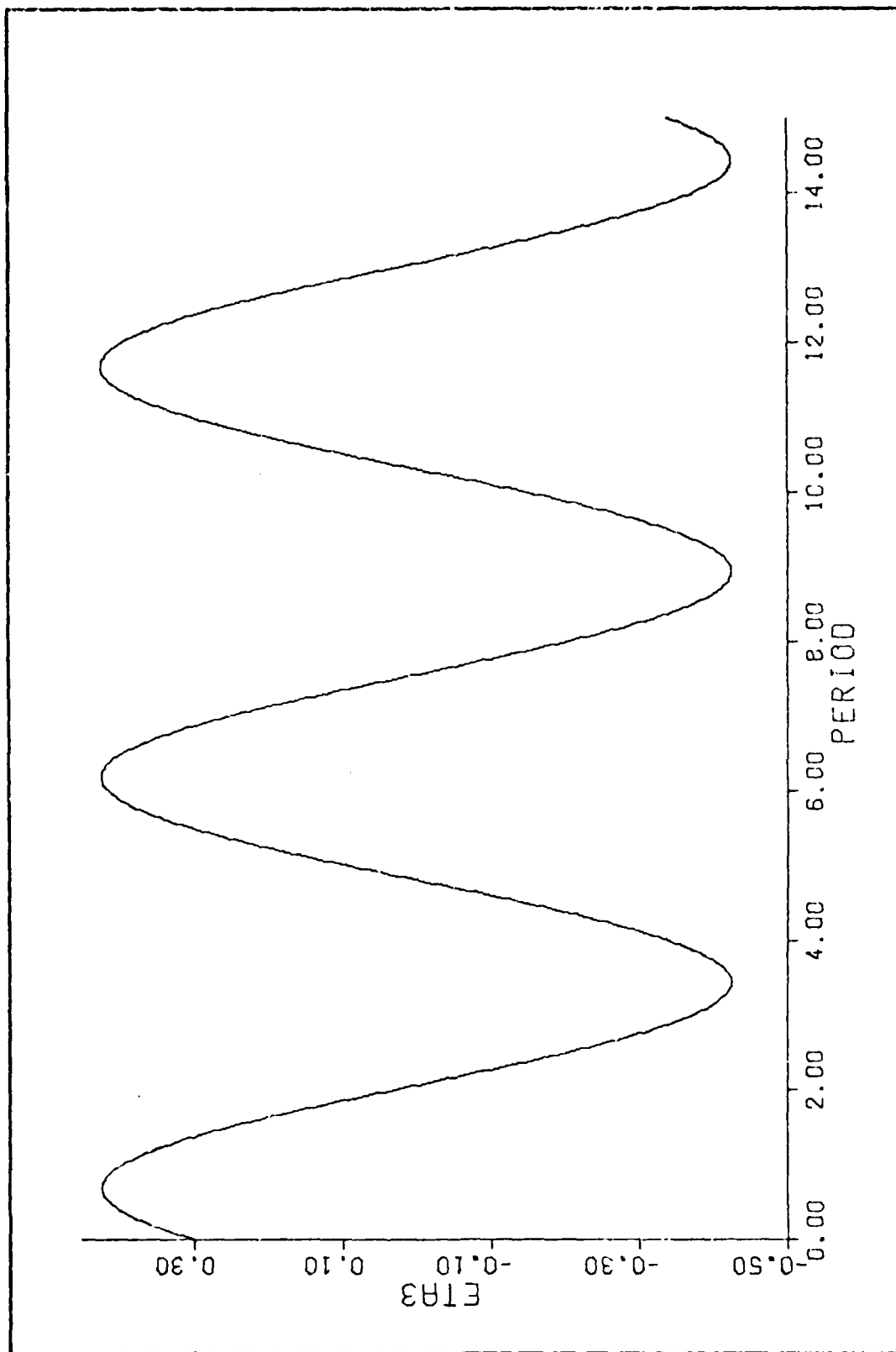


Figure 12. Uncontrolled Third Mode Response for Case 3

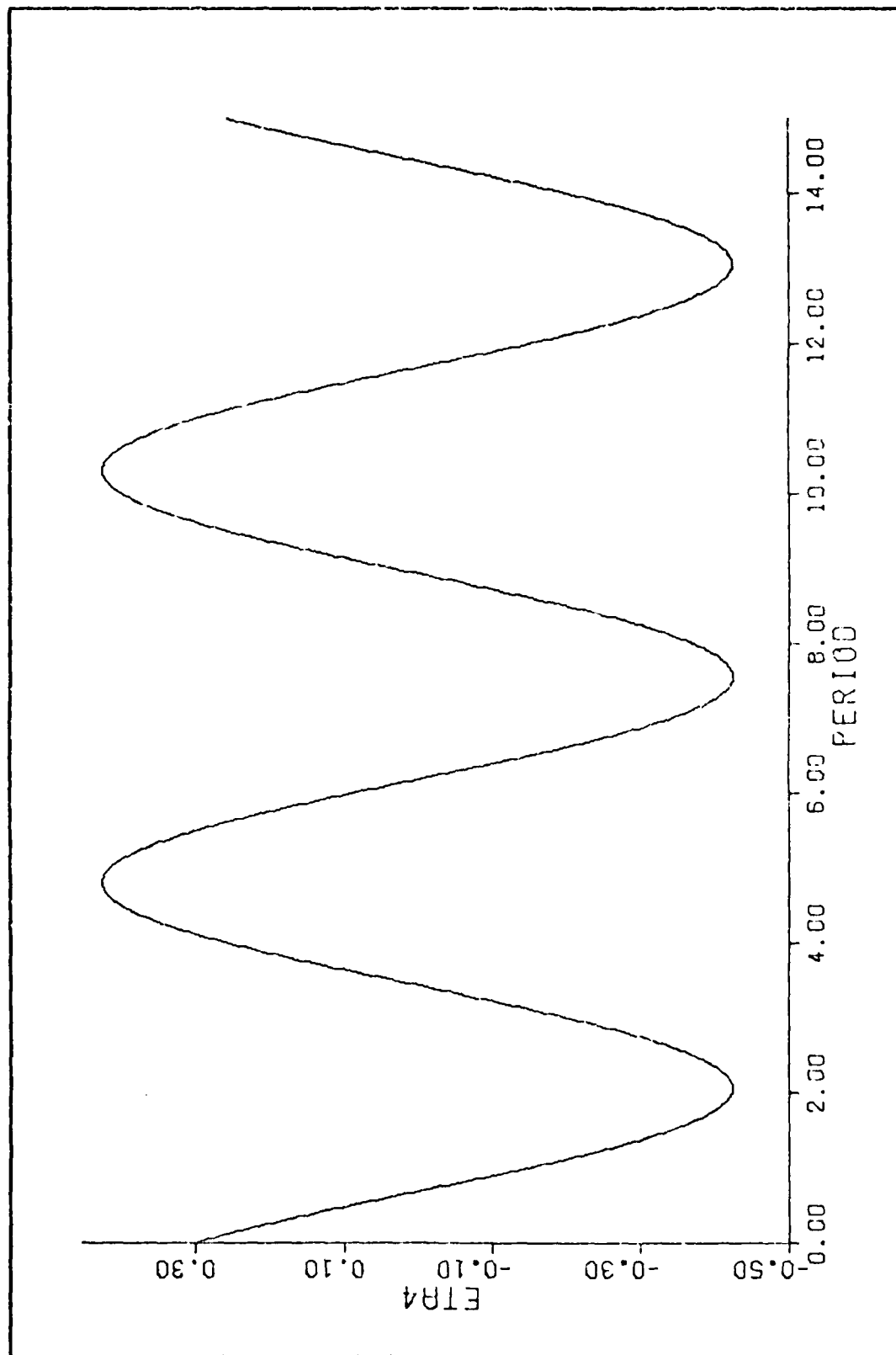


Figure 15. Uncontrolled Fourth Mode Response for Case 5

and fourth modes represent the typical low frequency, low damping oscillatory response of neutrally stable complex conjugate modes.

Thus, using Floquet theory as presented in Chapter III, the asymptotic stability of the five test cases is determined. By simulating the uncontrolled system, the stability of the uncontrolled systems is verified. In the following section, three of the unstable satellite cases are stabilized using the modal control theory of Chapter IV.

Satellite Stabilization and Verification

In this section, three of the four unstable satellite test cases are stabilized using modal control techniques and the control law developed in Chapter IV. These three cases, cases 1, 4, and 5, represent three different instability configurations. Case 1 has one unstable real characteristic exponent. Cases 4 and 5 both have two unstable modes. Case 4 has two unstable complex conjugate characteristic exponents and Case 5 has two unstable real characteristic exponents.

Single Mode Stabilization. To control Case 1, a controller must be utilized to control only the first mode. therefore, the results from the Single Controlled Mode section of the previous chapter are used. Since there is one controlled mode, the control law is

$$u(\tau) = k_1 n_1(\tau)$$

From Chapter IV, Equation (96) states that the closed-loop characteristic exponent is

$$\lambda_1^* = \lambda_1 + a_0 k_1$$

For this case, the uncontrolled system characteristic exponent is 0.6718 and the zero frequency portion of the first element of the mode-controllability matrix is 0.6198. Therefore, the gain required to move the characteristic exponent to zero is

$$0.0 = .6178 + .6198k_1$$

or

$$k_1 = -1.084$$

For the actual control of this system, the gain was set at -2.0, which results in a controlled characteristic exponent of -.5677. Table V contains the controlled system characteristic exponents for Case 1 based upon the numerical Floquet analysis described in Chapter III.

Table V
Case 1 Characteristic Exponents with
 $K = (-2.0, 0.0, 0.0, 0.0)$

	Uncontrolled	Controlled
λ_1	.6718	-.5677
λ_2	-.6718	-.6718
λ_3	0.0 + .3728i	0.0 + .3728i
λ_4	0.0 - .3728i	0.0 - .3728i

as expected, the simulation results, Figures 14 through 17, show a satellite with two exponentially decaying modes and two oscillating modes. Examining these responses, one notices a phenomenon that did not appear in the uncontrolled simulations. Each mode contains a transient response that decays rapidly. This transient response is due to the controller modifying the eigenvector associated with the controlled mode of the closed-loop monodromy matrix. This new eigenvector causes the initial transient to be displayed in all modal responses. With the addition of the controller, the characteristic exponents associated with the second, third, and fourth modes remained unchanged. Only the characteristic exponent for the first mode was altered. These results verify that modal control techniques only affect the characteristic exponents of the controlled modes. Also, the numerical results of this example validate the theory concerning the control of one mode in Chapter IV.

Multiple Controlled Mode Stabilization. Both cases 4 and 5 have multiple unstable modes. From Chapter IV, we found that when there are multiple controlled modes, the gains required for stabilization cannot be found directly by using a linear formula like the previous example. This problem with gain selection was due to the controlled-system coefficient matrix not being in a triangular form. Therefore, the solution to this type of problem is accomplished using a systematic search using various gain settings. This technique was used to stabilize both Case 4 and Case 5.

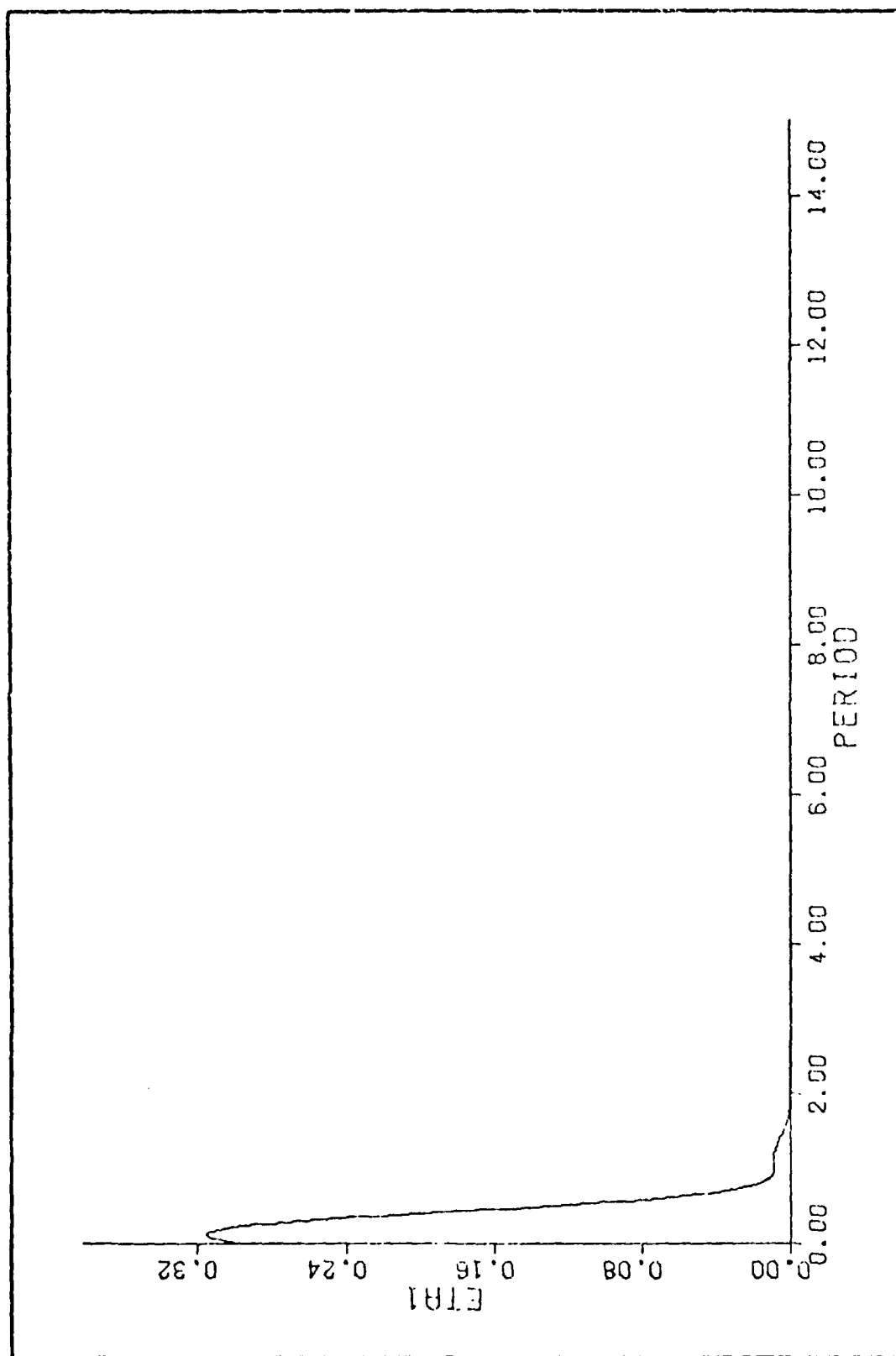


Figure 14. Controlled System First Mode Response for Case 1

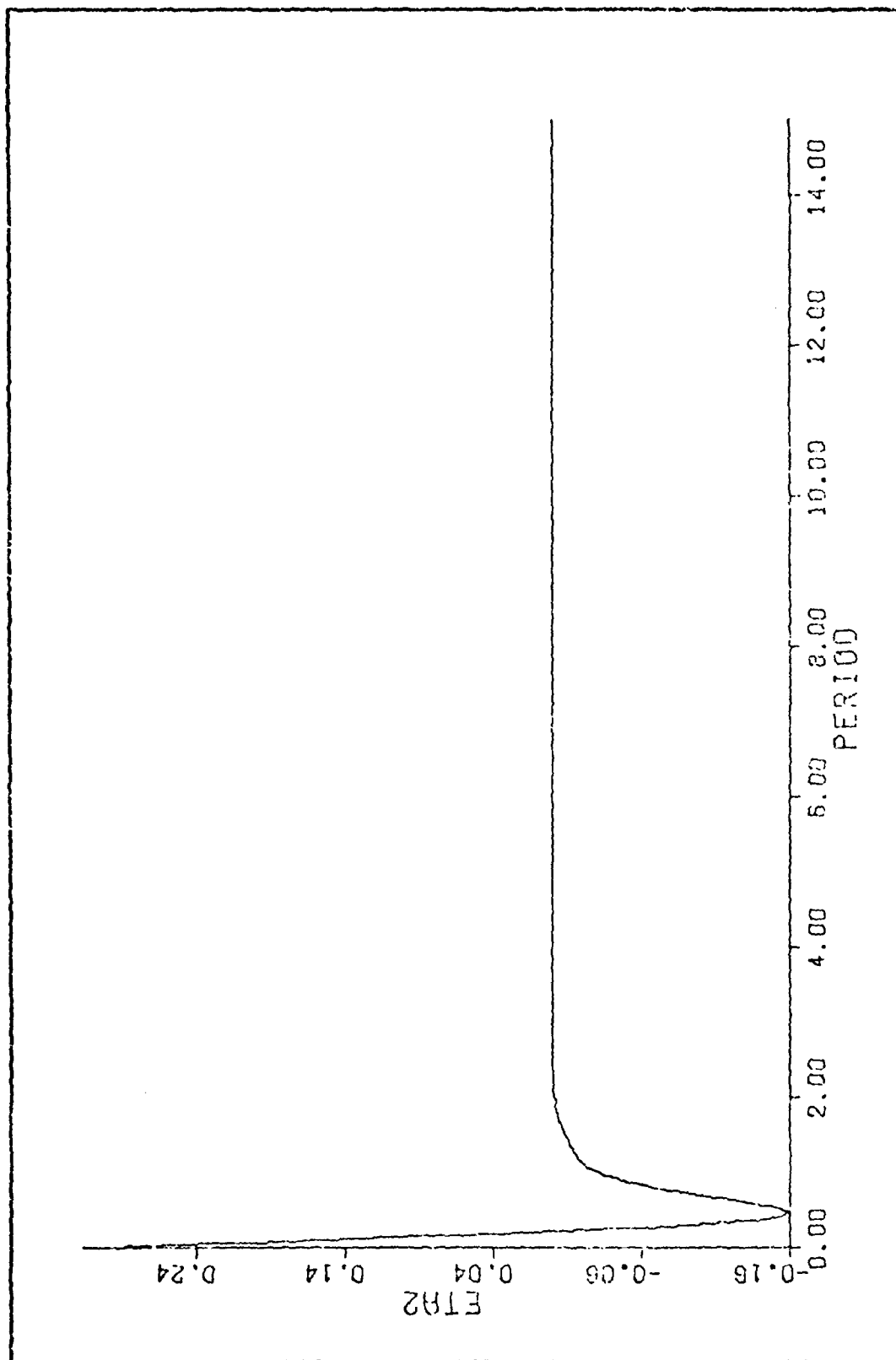


Figure 15. Controlled System Second Mode Response for Case 1

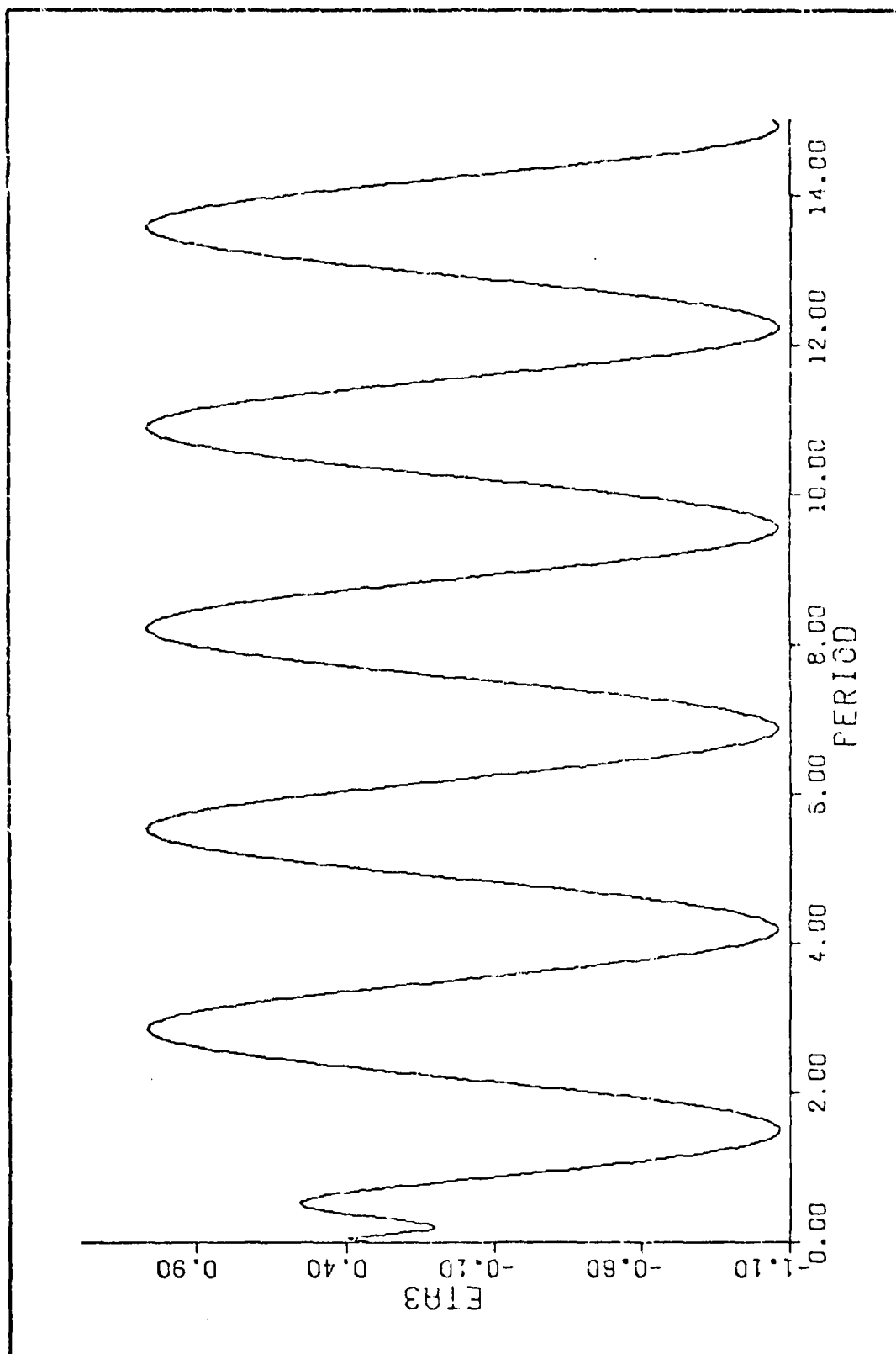


Figure 16. Controlled System Third Mode Response for Case 1

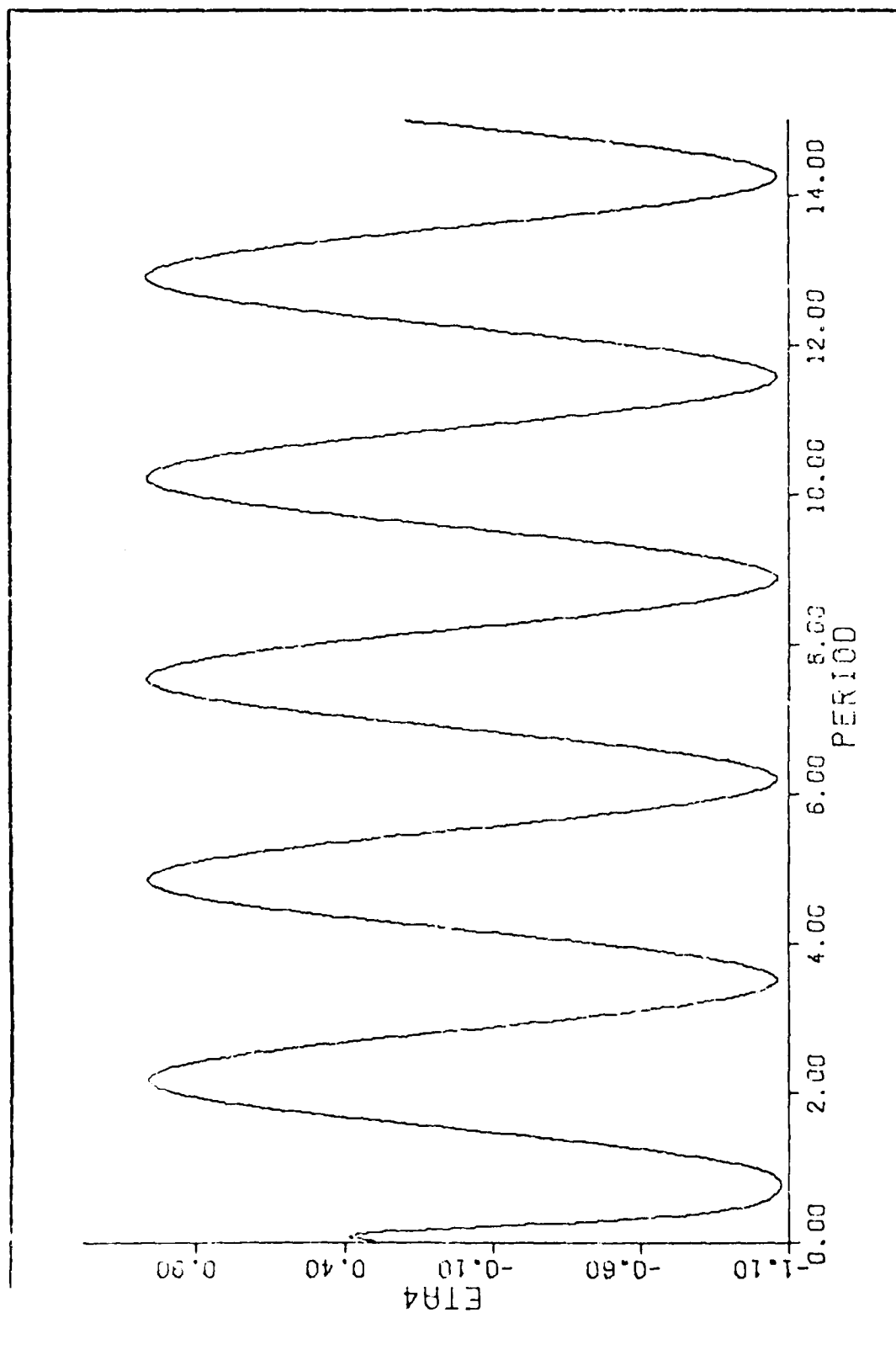


Figure 17. Controlled System Fourth Mode Response for Case 1

From Table IV, the unstable modes of Case 4 are the first and second modes. Therefore, the general control law necessary to control this case is

$$u(\tau) = k_1 \eta_1(\tau) + k_2 \eta_2(\tau)$$

Through the use of a systematic search procedure, the values of the two gains which provided adequate control and stable system characteristic exponents are $k_1 = 4.0$ and $k_2 = -10.0$. With these two gains, the two unstable characteristic exponents were moved to the left side of the complex plane. The results of the controlled-system monodromy matrix calculations are presented in Table VI. From these results, once again modal control techniques controlled only the modes requiring control.

Table VI
Case 4 Characteristic Exponents with
 $K = (4.0, -10.0, 0.0, 0.0)$

	Uncontrolled	Controlled
λ_1	.3557 + .1776i	-1.011 + .0146i
λ_2	.3557 + .1776i	-1.011 - .0146i
λ_3	-.3557 + .1776i	-.3557+ .1776i
λ_4	-.3557 - .1776i	-.3557- .1776i

These gain settings were used in a digital simulation of the modal variables. The results of the simulation are

illustrated in Figures 18 through 21. In this case, the oscillations in all modes damp out within three periods. This is due to the location, and therefore the existence of other than negligible damping, in the complex plane, of the controlled system characteristic exponents. Once again, the initial transients in all modes due to the new eigenvectors of the controlled system are apparent in these figures. Since all modes of this system damp out quickly and there are no highly oscillatory modal responses, this system presents an excellent system for simulation in physical variables. Therefore, with the initial conditions,

$$\bar{x}(0) = \begin{bmatrix} .05326 \\ .05326 \\ 0.0 \\ 0.0 \end{bmatrix}$$

and the control law given by

$$u(\tau) = KF^{-1}(\tau)\bar{x}(\tau)$$

this controlled system was simulated for fifteen periods using the physical variables. This simulation verifies that the linearized physical system is controlled with no unbounded growth in time of any of the state variables. Figures 22 through 25 illustrate the results of this simulation. The controller performed as expected, all oscillations of the state variables stopped after approximately three periods.

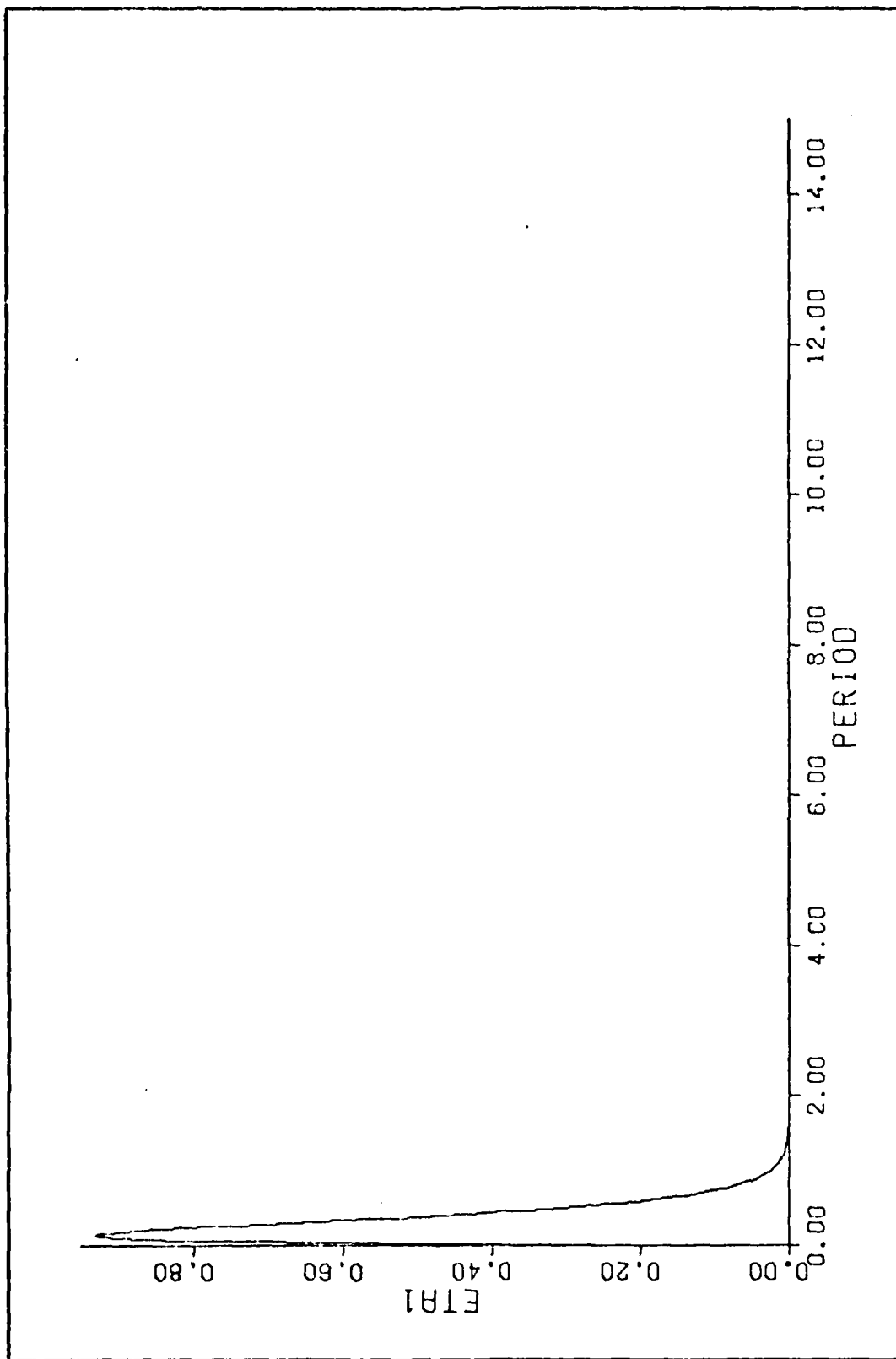


Figure 18. Controlled System First Mode Response for Case 4

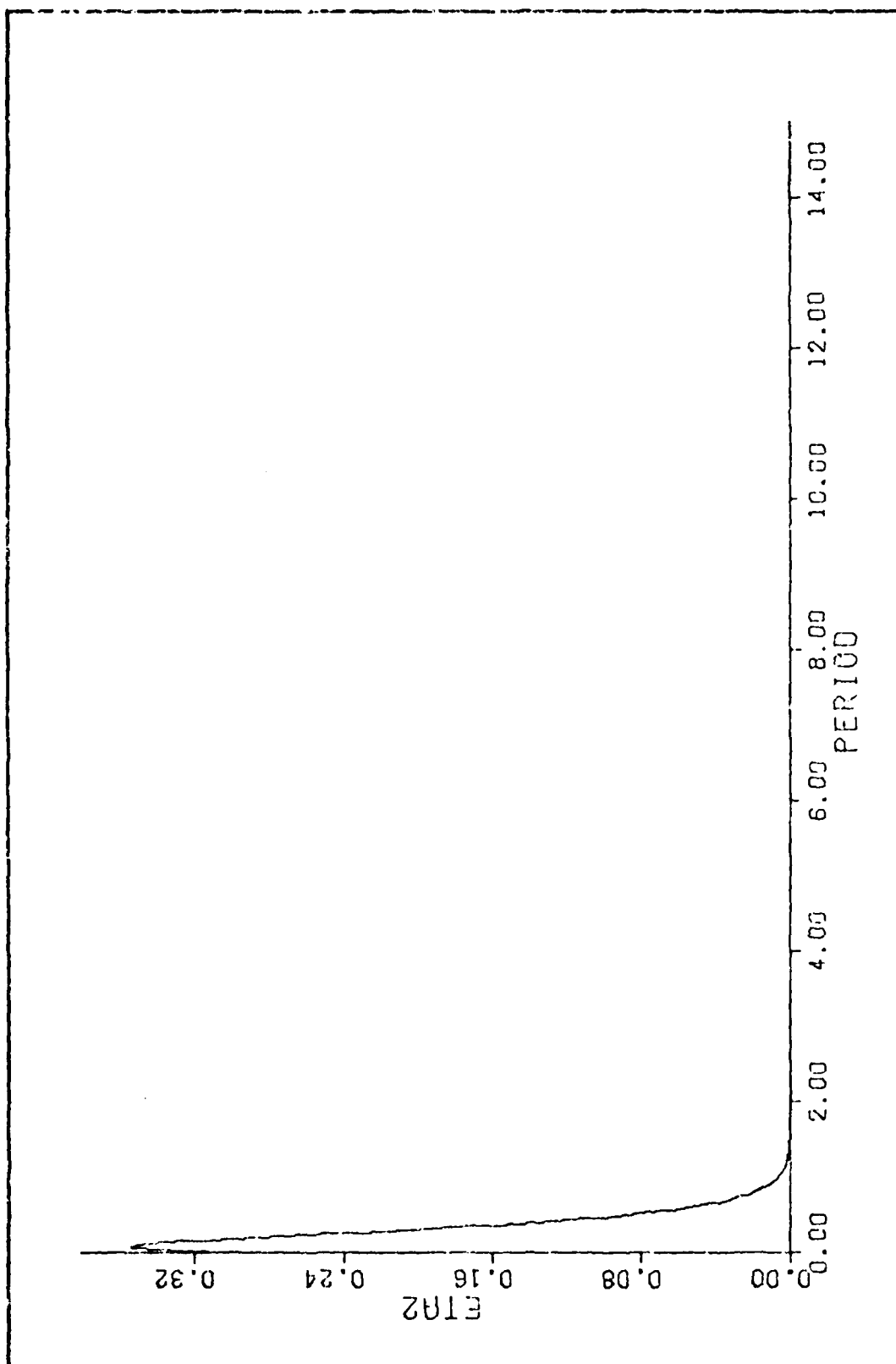


Figure 19. Controlled System Second Mode Response for Case 4

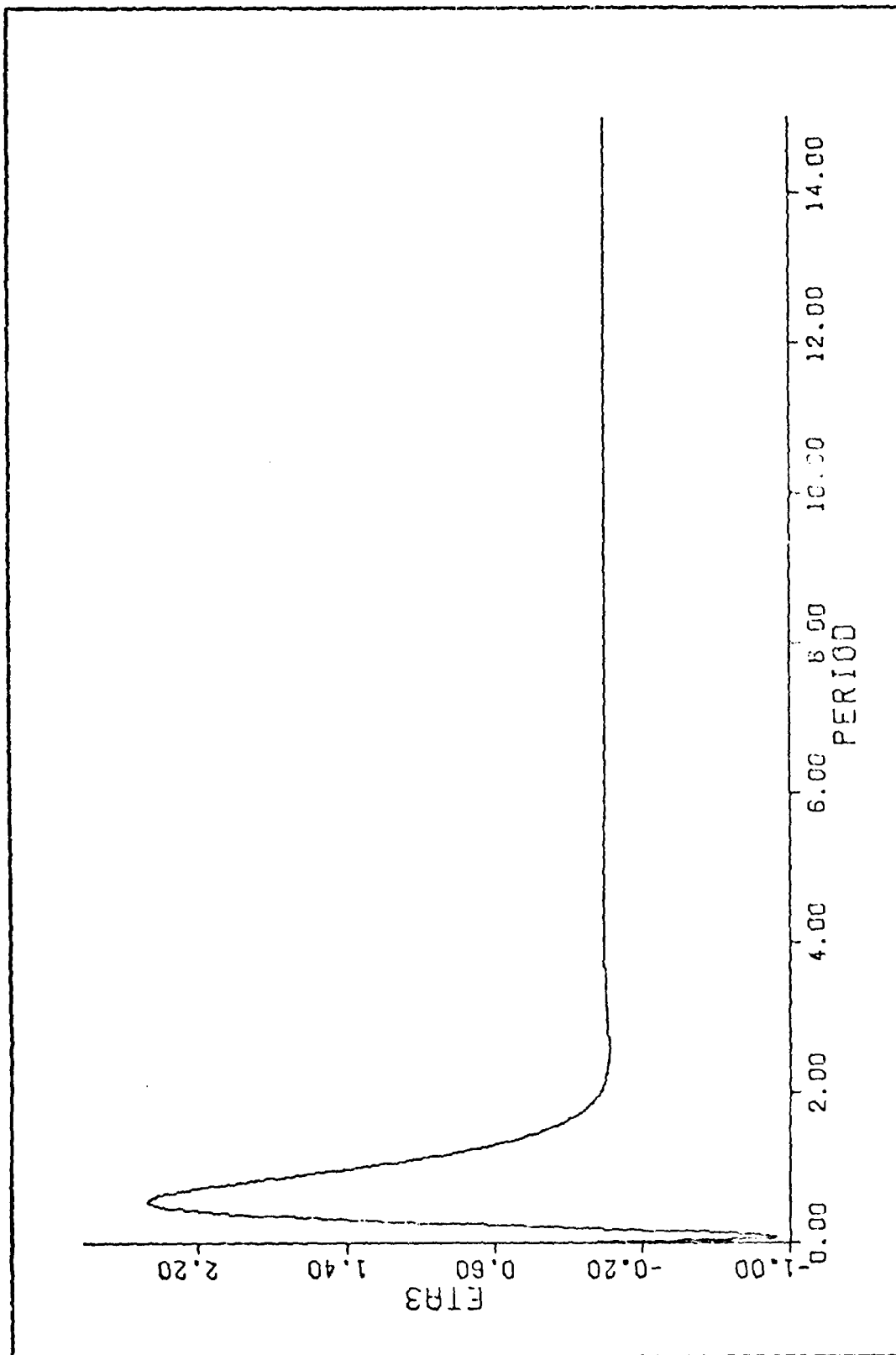


Figure 20. Controlled System Third Mode Response for Case 4

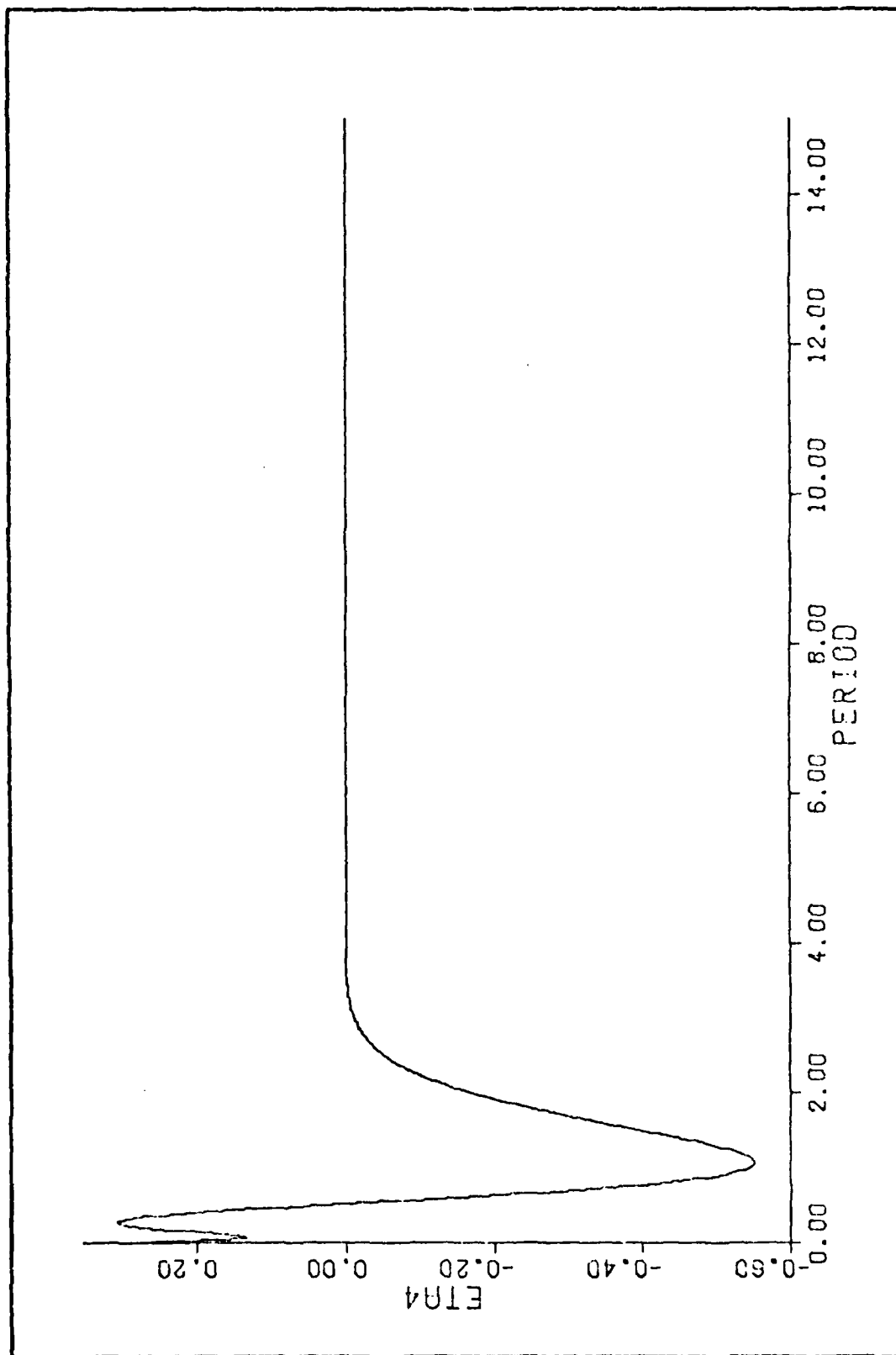


Figure 21. Controlled System Fourth Mode Response for Case 4

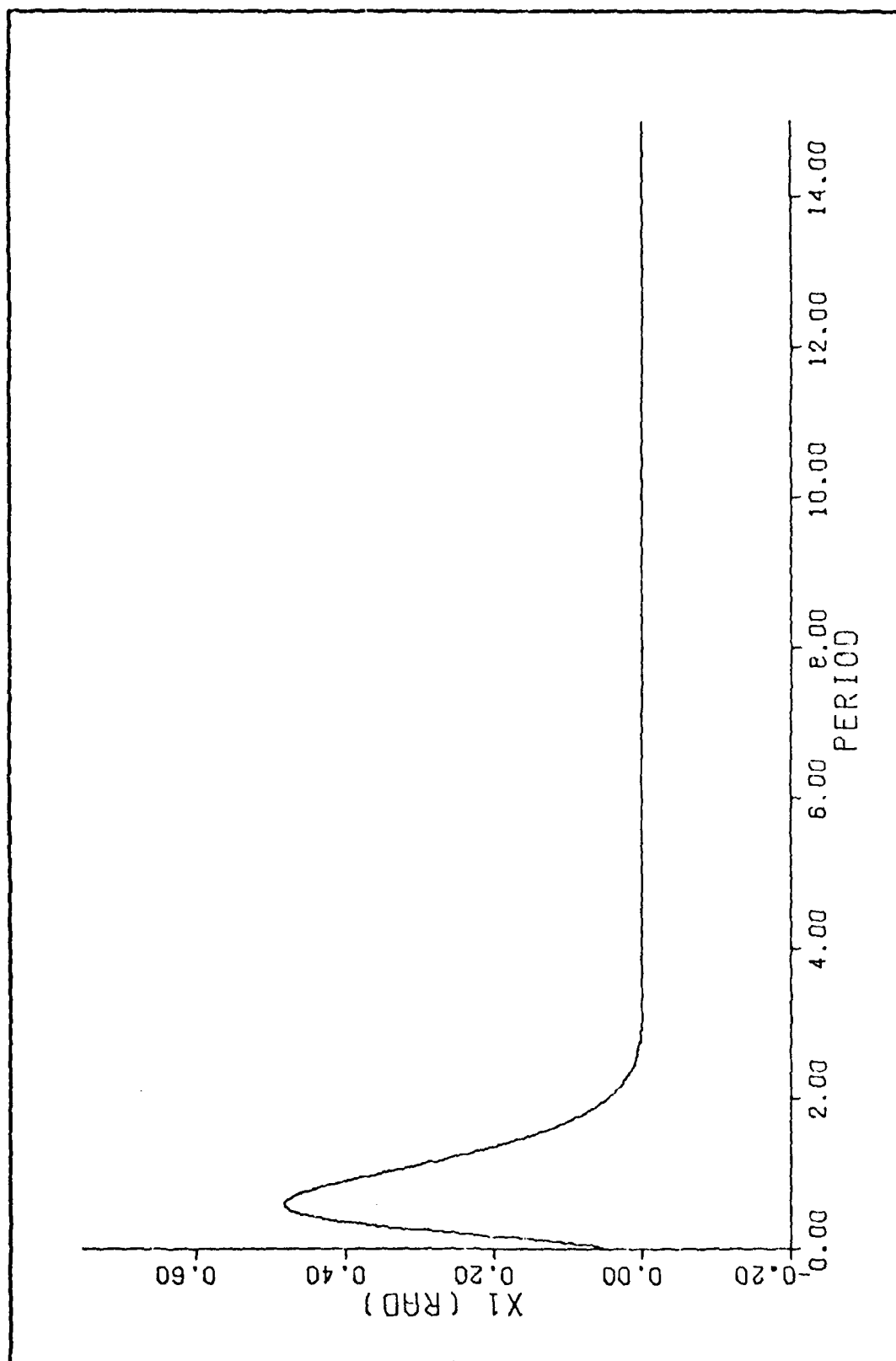


Figure 22. Controlled $x_1(\tau)$ Response for Case 4

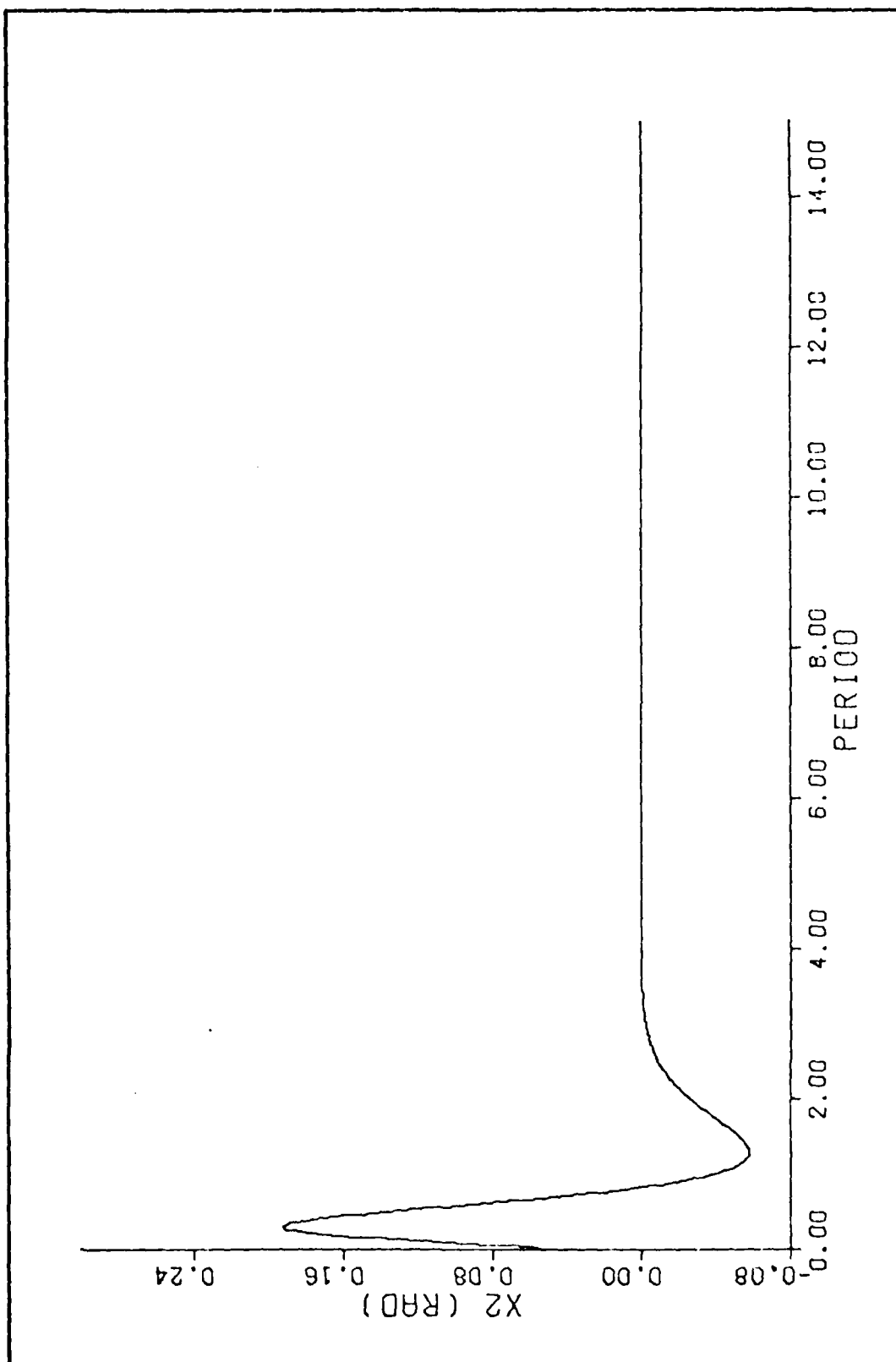


Figure 25. Controlled $x_2(\tau)$ Response for Case 4

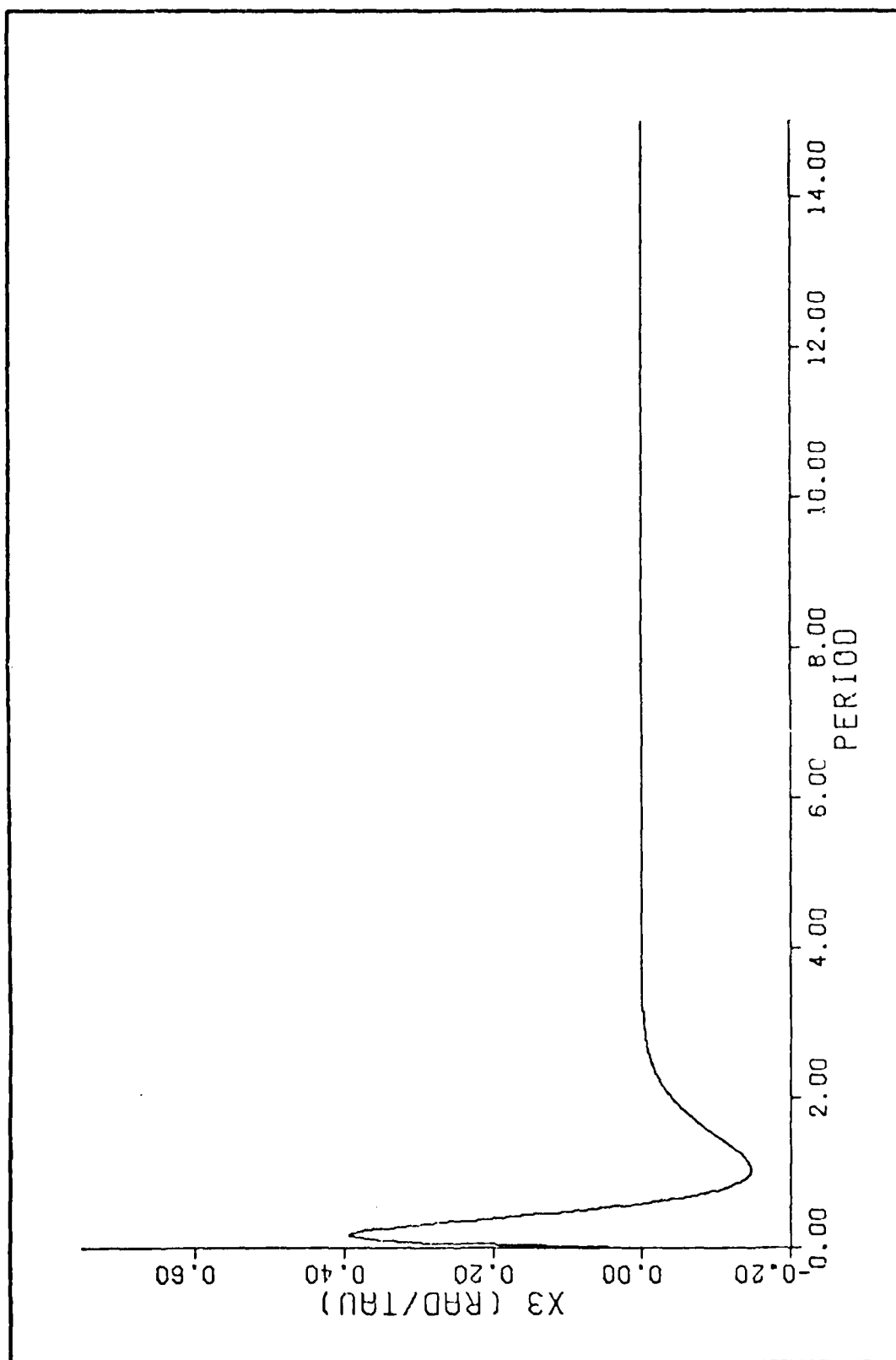


Figure 24. Controlled $x_3(\tau)$ Response for Case 4

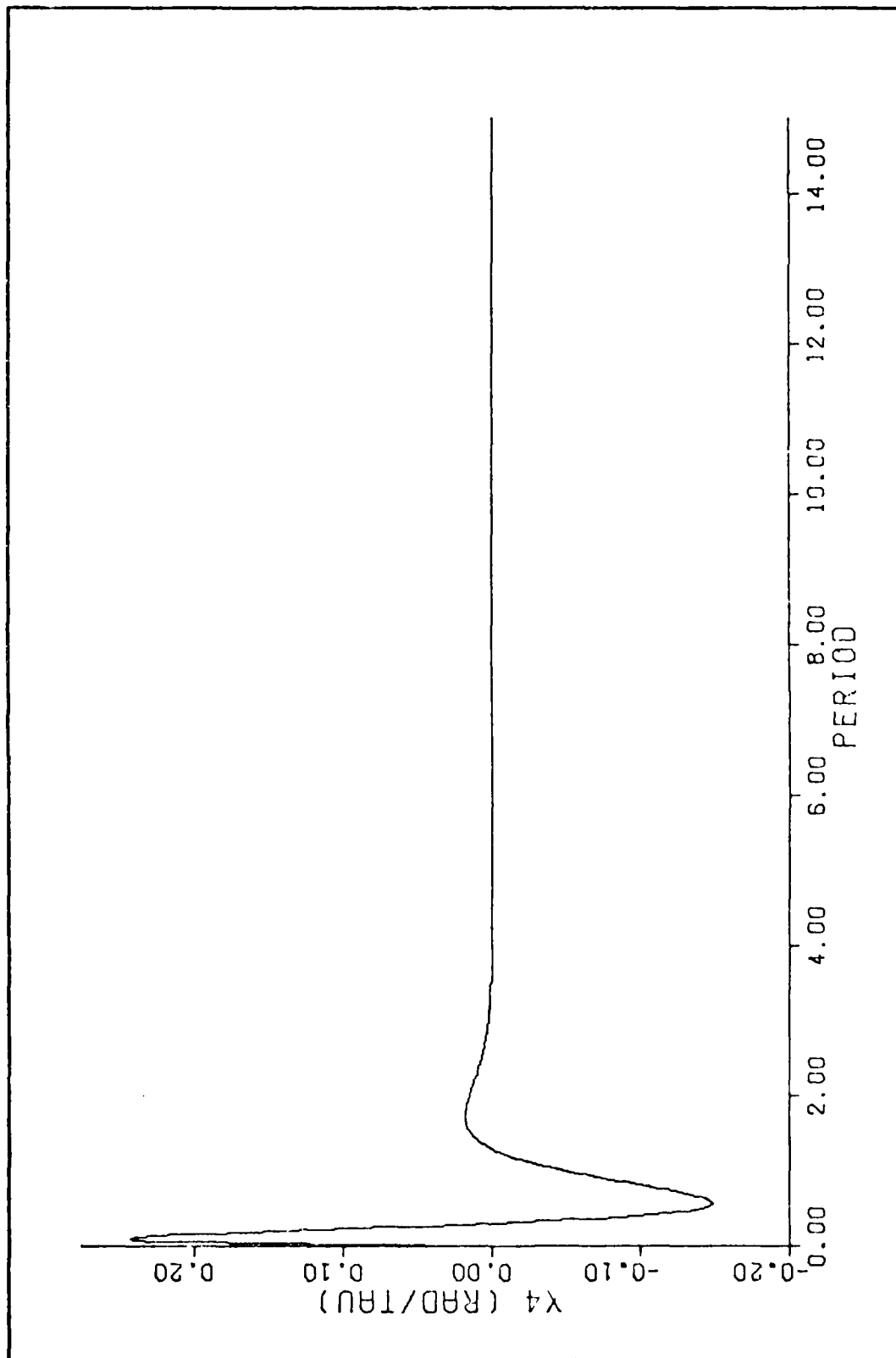


Figure 25. Controlled $x_4(\tau)$ Response for Case 4

The final test case to be controlled, Case 5, has two unstable real characteristic exponents. Thus, since there are two modes requiring control, the same techniques used in the control of Case 4 are used. From Table IV, the unstable modes are the first and third modes. Therefore, the scalar control law for the control of this system is

$$u(\tau) = k_1 \eta_1(\tau) + k_3 \eta_3(\tau)$$

Using a systematic search technique, the gains that provided adequate control for this satellite are $k_1 = -1.4$ and $k_3 = -.01$. Table VII contains the results of the closed-loop analysis using Floquet theory.

Table VII
Case 5 Characteristic Exponents with
 $K = (-1.4, 0.0, -.01, 0.0)$

	Uncontrolled	Controlled
λ_1	.8265	-.0582 + .0971i
λ_2	-.8265	-.8265
λ_3	.2128	-.0582 - .0971i
λ_4	-.2128	-.2128

From these results, the control law provides adequate control for the unstable modes to bring them under control. Figures 26 through 29 present the results of simulating the

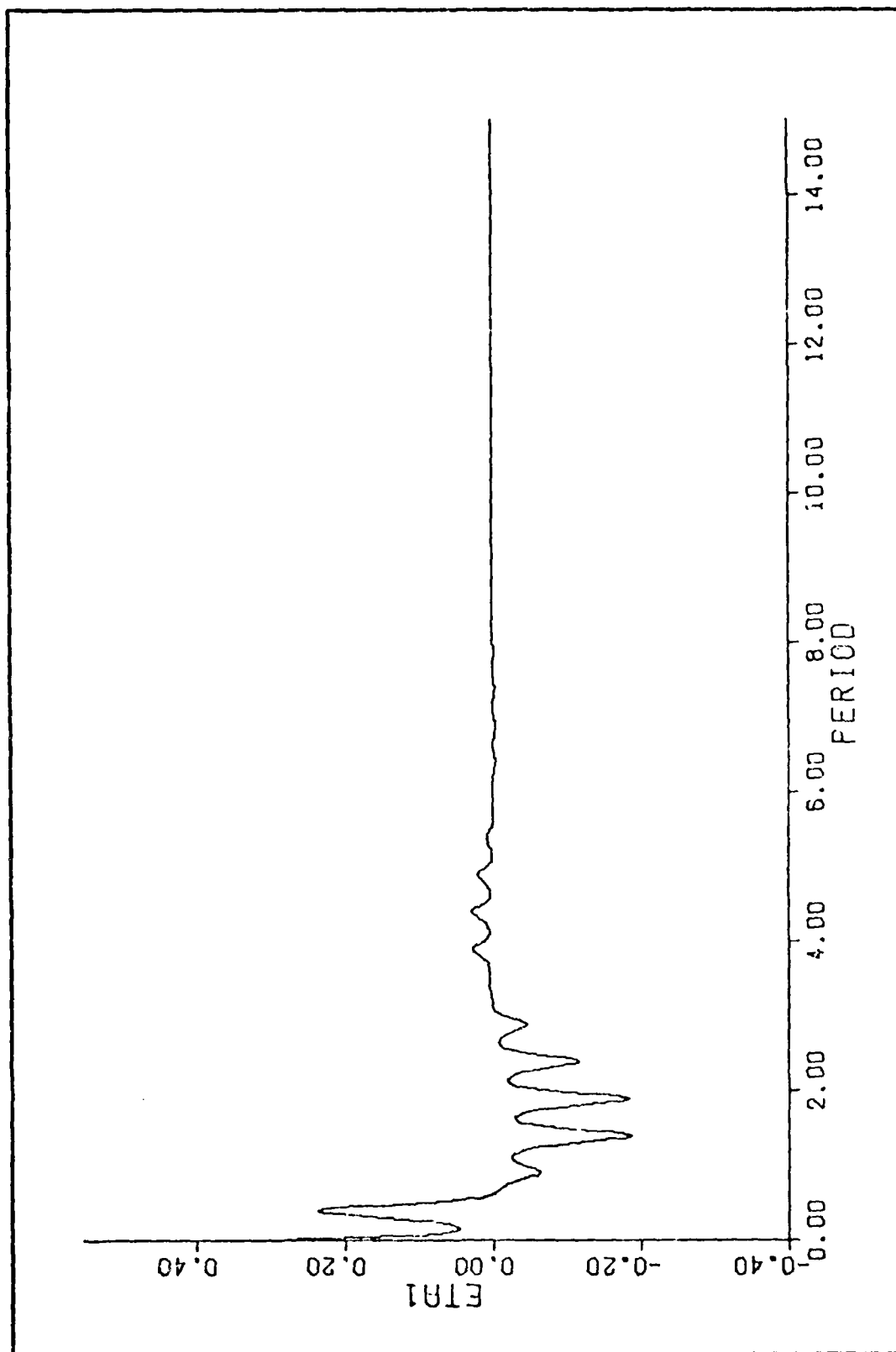


Figure 26. Controlled System First Mode Response for Case 5

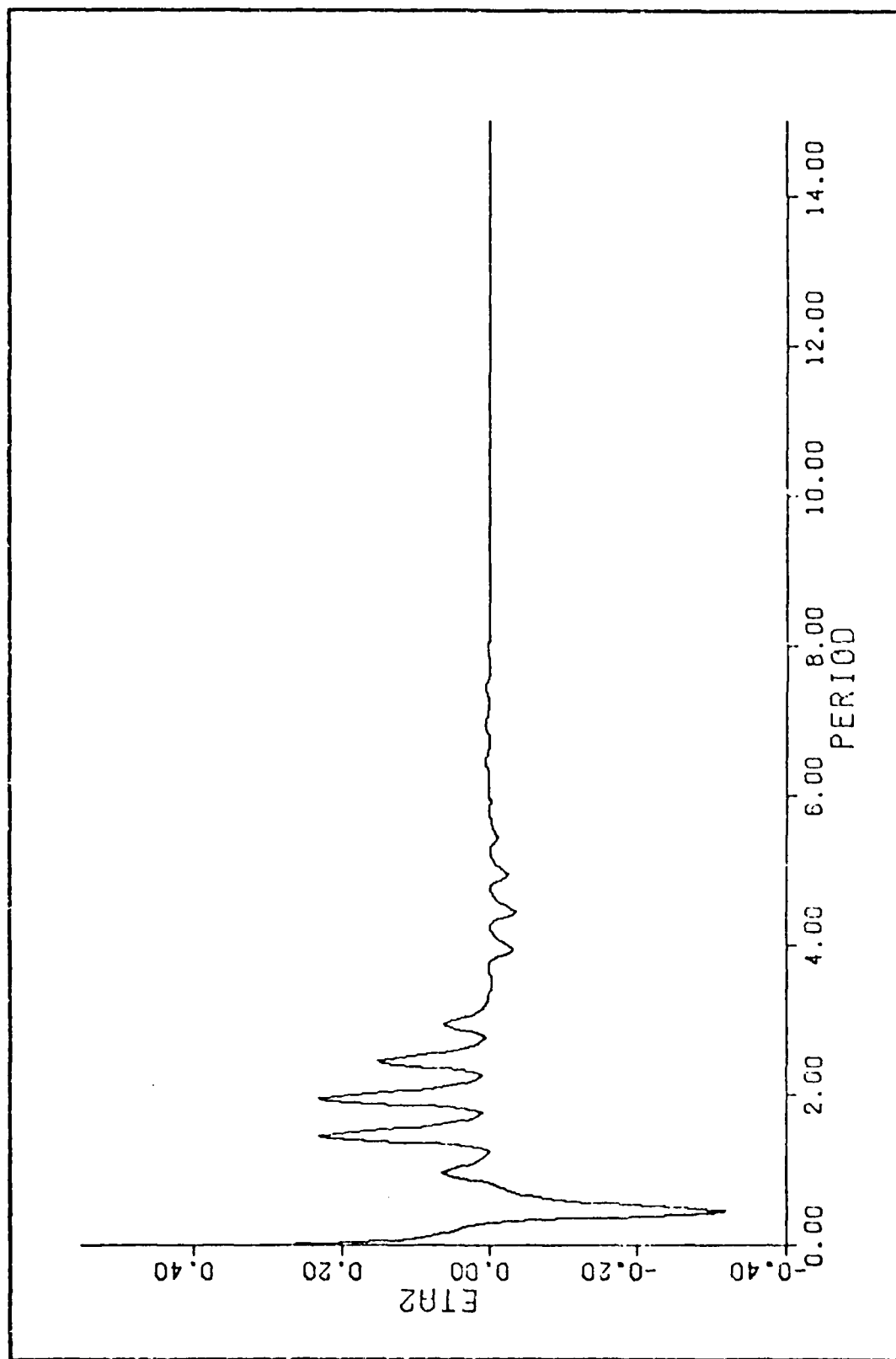


Figure 27. Controlled System Second Mode Response for Case 5

AD-A111 067 AIR FORCE INST OF TECH WRIGHT-PATTERSON AFB OH SCH00--ETC F/0 22/3
ACTIVE CONTROL OF LINEAR PERIODIC SYSTEMS.(U)

DEC 81 6 5 YEAKEL

UNCLASSIFIED AFIT/GA/AA/81D-12

NL

2 OF 2

ADA
11-DB

END

DATE

FILED

103-82

DTIC

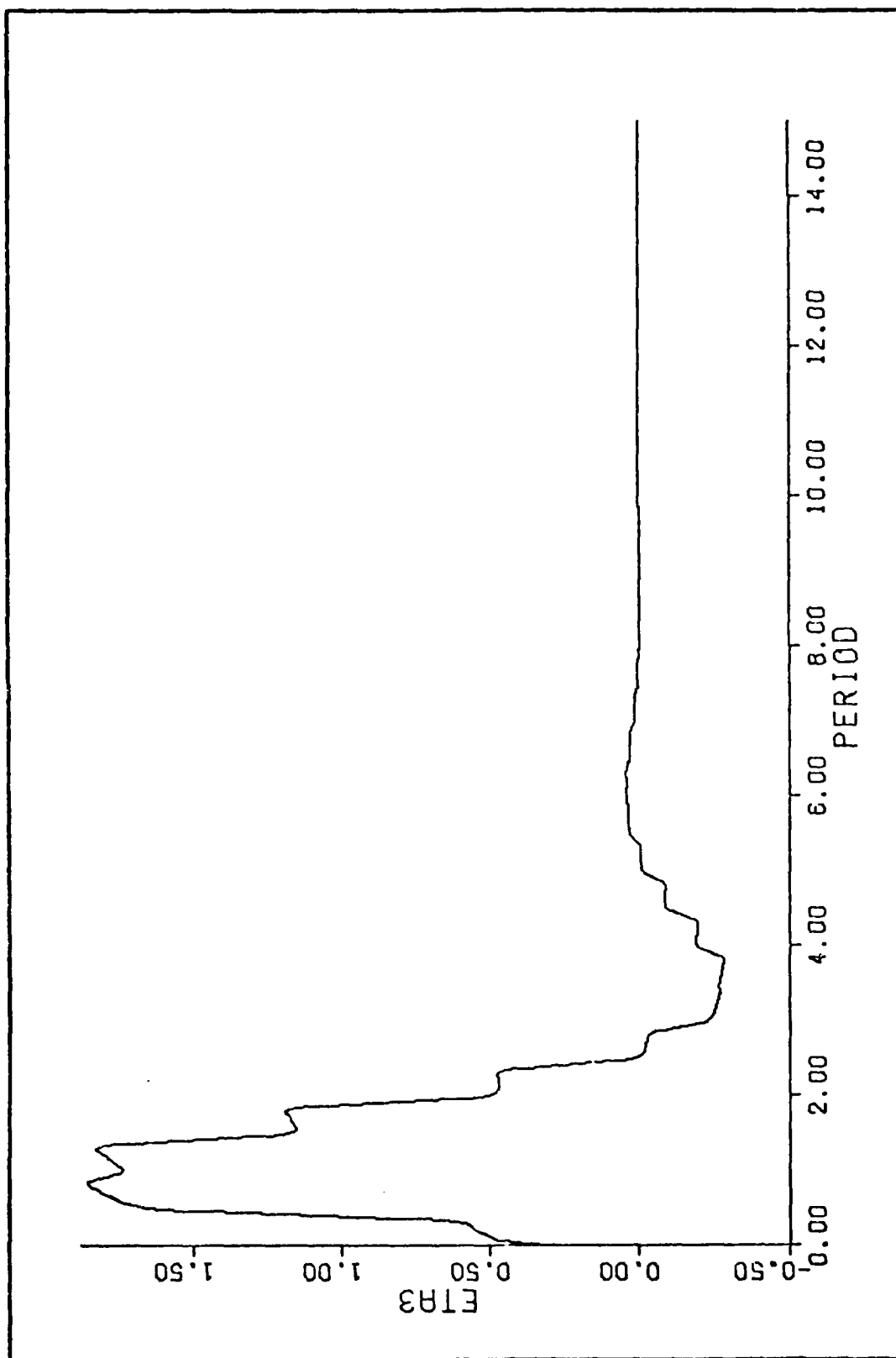


Figure 28. Controlled System Third Mode Response for Case 5

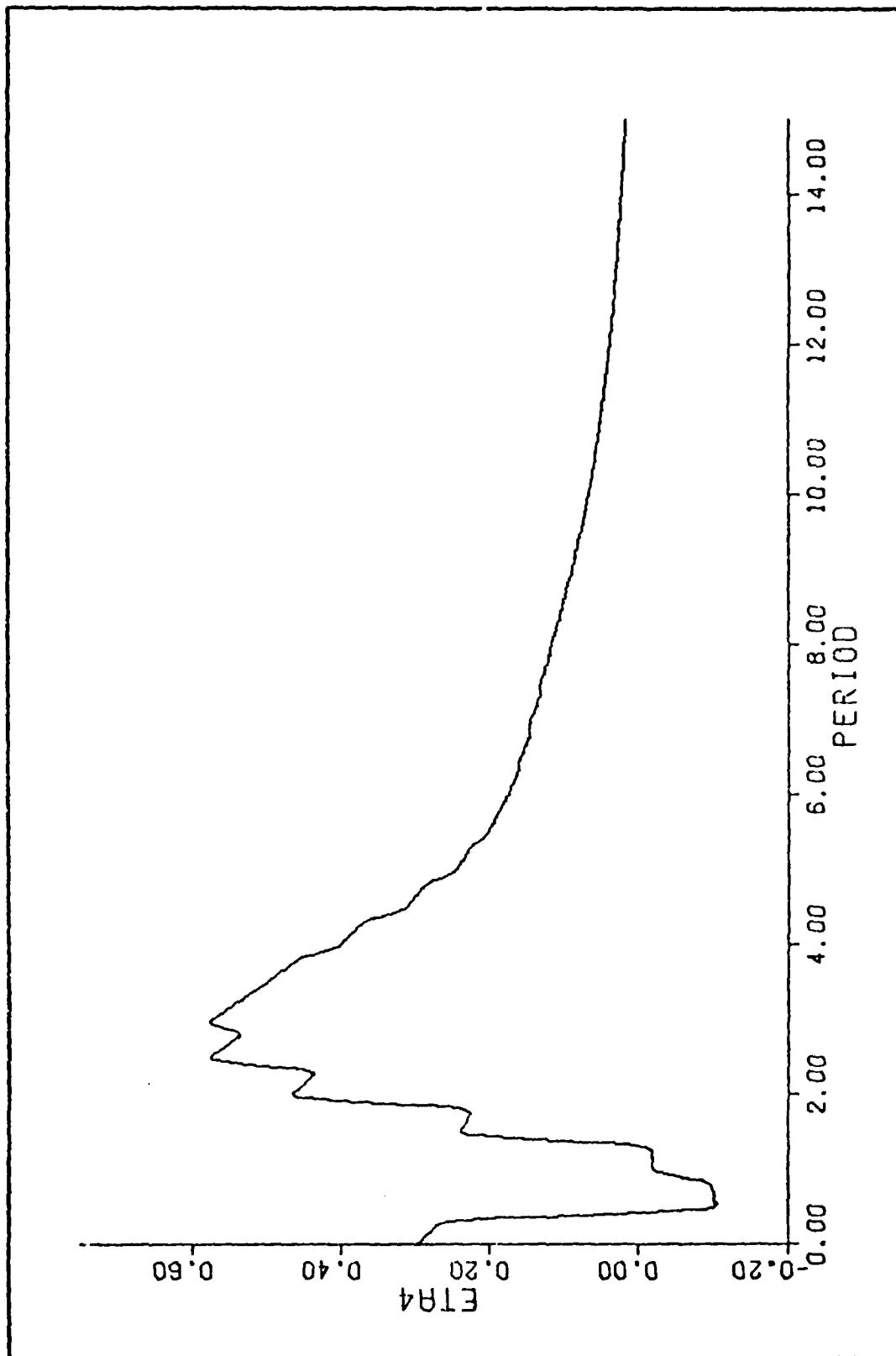


Figure 29. Controlled System Fourth Node Response for Case 5

controlled system over fifteen periods. In this case, all modes were controlled and eventually reduced to zero. The previously mentioned transient responses are more pronounced in this case than in the other two cases. These transient response characteristics are due to the eigenvectors of the closed-loop system monodromy matrix. During this study, no attempt was made to specify the desired transient response characteristics of the controlled systems.

With these numerical and graphical results, the implementation and verification of the control law and associated theoretical developments are complete. As presented in the examples, modal control provided the required control over only the controlled modes and only the initial transients of the other modes were affected. Also, the generalizations made concerning stable gravity gradient satellites in Chapter I were demonstrated in the various examples. During the completion of these investigations, numerical problems associated with the computations of the $F^{-1}(\tau)$ matrix were encountered. In the following section, these numerical problems and their effects on the controlled system are addressed.

Numerical Problems Associated with $F^{-1}(\tau)$ Computations

One of the basic elements in the closed-loop system, from Equation (74), is the $F^{-1}(\tau)$ matrix. This matrix, which appeared during the diagonalization and subsequent control processes, is periodic with period T . As such, by finding $F^{-1}(\tau)$ over one period is equivalent to finding this matrix

over all τ . Therefore, to ease computational burden, the method of computing the $F^{-1}(\tau)$ matrix for the closed-loop stability analysis and subsequent digital simulations was to compute $F^{-1}(\tau)$ for m evenly spaced points during one period. Using these m $F^{-1}(\tau)$ matrices, a harmonic analysis was completed on all sixteen elements (Ref. 2: 108-109). The results of this harmonic analysis were $\frac{m}{2} + 1$ cosine Fourier coefficients and $\frac{m}{2} - 1$ sine Fourier coefficients. With these coefficients, the $F^{-1}(\tau)$ matrix can be computed at any τ . Using this technique, the closed-loop system, in either modal or state variables, is integrated. Using Case 3, it is shown how this computational technique does not insure the precise computations of the $F^{-1}(\tau)$ matrix required to satisfy Equation (77). From Table IV, Case 3 has one unstable characteristic exponent. Thus, since there is one unstable mode, the controlled characteristic exponent, λ_1^* , is found by using Equation (96). For this case, the zero frequency portion of the first element of the mode-controllability matrix, a_0 , is -0.2187. Using Equation (96), the theoretical value for λ_1^* , is found, and by finding the characteristic exponents of the closed-loop system monodromy matrix, the numerically derived value of λ_1^* is found. Comparing these two values, the effects of these numerical problems associated with the $F^{-1}(\tau)$ can be ascertained. These computations were carried out for five gain settings, the results are tabulated in Table VIII. From Table VIII, one notices that as the gain is increased, the theoretically

Table VIII

Theoretical and Computed Values of the Characteristic Exponents for Case 3

Gain (k_1)	10^{-6}	10^{-3}	10^{-1}	10^0	10^1
Theoretical					
λ_1^*	.125818	.12560	.10395	-.07287	-2.06101
Computed					
λ_1^*	.125818	.12560	.10395	-.09138	-.08505 +.5000i
λ_2	0.0 +.181856i	0.0 +.181856i	0.0 +.181856i	-4.0 x 10^{-4} +.18204i	-.069836 +.17457i
λ_3	0.0 -.181856i	0.0 -.181856i	0.0 -.181856i	-4.0 x 10^{-4} -.18204i	-.069836 -.17457i
λ_4	-.125818	-.125818	-.125818	-.12741	-1.0639 +.5000i

and numerically computed characteristic exponents diverge. In fact, there should be no variation in the characteristic exponents of the modes which are uncontrolled. However, with a gain of 1.0, there are apparent variations in the uncontrolled characteristic exponents.

These variations are due to the loss in accuracy of $F^{-1}(\tau)$. To examine this loss of accuracy, the $F^{-1}(\tau)$ matrix at $\tau = \pi$ was computed using the Fourier series for each element and by integrating Equation (77) as presented in Chapter IV. The results are presented in Figure 30. Examining these two matrices, one notes that there are significant differences. The accuracy of the Fourier series can be improved by increasing the number of function evaluations used in the harmonic analysis. An increased number of function evaluations was tried, but the resulting $F^{-1}(\tau)$ matrix was still too inaccurate. Therefore, these inaccuracies are due to using the Fourier coefficients to compute the $F^{-1}(\tau)$ matrix. There are many possible causes for these numerical problems, among these are truncation errors and finite wordlength of the computer. However, no definite cause for these problems was determined.

This completes the discussion of the results compiled during this study. Consisely, the results indicate the ability to control unstable satellites under the influence of a gravity gradient. However, numerical problems in the computation of the mode-controllability matrix were encountered.

Using Fourier Coefficients:

$$F^{-1}(\tau) = \begin{bmatrix} -1.07163 & -0.42118 & 0.68055 & -0.25558 \\ 0.62281 & -0.24466 & 0.39587 & 0.14898 \\ 0.52601 & -0.68481 & -0.73827 & 0.47968 \\ -2.43237 & -0.14823 & -0.15884 & -2.22316 \end{bmatrix}$$

Using Analytical Techniques:

$$F^{-1}(\tau) = \begin{bmatrix} -1.07175 & -0.42112 & 0.68092 & -0.25598 \\ 0.62275 & -0.24470 & 0.39565 & 0.14874 \\ 0.52672 & -0.68480 & -0.73806 & 0.481138 \\ -2.43222 & -0.14830 & -0.15984 & -2.22281 \end{bmatrix}$$

Figure 30. $F^{-1}(\tau)$ Calculated at $\tau = \pi$
using the Fourier Coefficients
and Analytical Techniques

CHAPTER VI

CONCLUDING REMARKS AND RECOMMENDATIONS

The problem that this study addresses is the control of satellite attitude motion while the satellite is under the influence of a gravity gradient. Since the linearized equations describing the attitude motion are periodic, the controller must control the location, in the complex plane, of the characteristic exponents. As seen in the previous chapter, the modal control scheme and the control law developed during this study provide adequate control over the satellite attitude motion. The control law demonstrated that, in general, it only controls the modes requiring control. Therefore, the modal control techniques provide a viable control scheme for the attitude control of unstable satellites described by linear periodic systems.

During this study, it became apparent that there are two areas requiring additional work. First, a problem was encountered numerous times with the computations of the mode-controllability matrix. The result of this computational problem is inaccurate or fictitious results when the computing the stability characteristics of the controlled system. The second area requiring additional study is in the gain selection techniques for stabilizing a satellite with more than one unstable mode. In this study, a systematic

search procedure was used, but in general, one would like to select the gains directly. With additional work in these areas, the modal control technique and the control law presented in this study will provide an extremely flexible method for controlling periodic systems whose asymptotic stability characteristics are undesirable.

Recommendations for Future Studies

The recommendations for future studies consist of two levels. The first level recommendations are future study efforts involving the same techniques used during this study. The second level recommendations are for future studies for developing a control scheme for on-line applications in a real world environment.

The first level recommendations are ways to obtain more accurate calculations of the mode-controllability matrix. There is one basic means of accomplishing this. This means is by using double precision arithmetic $F^{-1}(\tau)$ calculations. All computations in this study were completed using single precision arithmetic. By increasing the precision, more accurate results may be obtained.

The second level recommendations are possible methods of achieving acceptable results in a real world environment. The first method is to use a Kalman filter to provide state estimations. Using sensor models, which take noise corrupted measurements of output variables, the Kalman filter can then be used to generate state estimates. These state

estimates are then used as the feedback variables instead of the actual states. This technique provides a more realistic application of the control techniques presented in this study. In the real world, sensors would be used to measure the angular rates and angles. This data would then be used to activate the controller. The second method is to design an optimal controller using LQG design techniques. LQG design techniques provide an optimal controller for a problem described by linear models with quadratic cost criterion and Gaussian noise models. This is a reasonable choice since the linear periodic system models can be assumed to be corrupted by noise. This noise can be due to such items as atmospheric drag, gravity anomalies, solar wind, etc. Under these assumptions, an optimal stochastic regulator can be designed.

BIBLIOGRAPHY

1. Bate, Roger R., Donald D. Mueller and Jerry E. White. Fundamentals of Astrodynamics. New York: Dover Publications, Inc., 1971.
2. Brouwer, D., and G.M. Clemence. Methods of Celestial Mechanics. New York: Academic Press, 1961.
3. Erugin, Nikolay P. Linear Systems of Ordinary Differential Equations with Periodic and Quasi-Periodic Coefficients: Mathematics in Science and Engineering. Volume 28, edited by Richard Bellman. New York: Academic Press, 1966.
4. "Forecasting the 80s," Astronautics and Aeronautics, 19 (7-8): 20-36 (July/August, 1981).
5. Hartman, Philip. Ordinary Differential Equations. New York: John Wiley and Sons, Inc., 1964.
6. Kane, T.R., and D.J. Shippy. "Attitude Stability of a Spinning Unsymmetrical Satellite in a Circular Orbit," The Journal of the Astronautical Sciences, 10 (4): 114-119 (Winter 1963).
7. Kane, T.R., and P.M. Barba. "Attitude Stability of a Spinning Satellite in an Elliptic Orbit," Journal of Applied Mechanics: 402-405 (June, 1966).
8. Kaplan, Marshall H. Modern Spacecraft Dynamics and Control. New York: John Wiley and Sons, Inc., 1976.
9. Kaplan, Wilfred. Advanced Calculus. Reading, Massachusetts: Addison-Wesley Publishing Company, 1972.
10. Kreyszig, Erwin. Advanced Engineering Mathematics. New York: John Wiley and Sons, Inc., 1972.
11. Lindh, Kenneth G., and Peter W. Likins. "Infinite Determinant Methods for Stability Analysis of Periodic-Coefficient Differential Equations," AIAA Journal, 8 (4): 630-636 (April, 1970).
12. Meirovitch, Leonard. Methods of Analytical Dynamics. New York: McGraw-Hill Book Company, 1970.

13. Porter, Brian, and Roger Crossley. Model Control: Theory and Applications. London: Taylor and Francis, 1972.
14. Shelton, William L. Model Control of a Satellite in Orbit about L3. MS thesis. Wright-Patterson AFB, Ohio: Air Force Institute of Technology, December, 1980.

VITA

Glenn S. Yeakel was born on May 28, 1956 in Allentown, Pennsylvania. Spending all of his childhood years in the Allentown area, he graduated from Emmaus High School in June, 1974. Upon graduating from high school, he accepted an appointment to the U.S. Air Force Academy in July, 1974. He graduated from the U.S. Air Force Academy in 1978 with a Bachelor of Science Degree in Aeronautical Engineering and received a regular commission in the U.S. Air Force.

In July, 1978, G.S. Yeakel was assigned as a Project Engineer in the Air Force Flight Dynamics Laboratory, Wright-Patterson AFB, Ohio. While assigned there, he was active in the development of advanced flight control systems for fighter control systems for fighter and transport aircraft, and he directed programs in the exploratory development of advanced flight and fire control technology for fighter aircraft.

In September, 1980, Yeakel was reassigned to the Air Force Institute of Technology, at Wright-Patterson AFB. While assigned there, he pursued a Master of Science Degree in Astronautical Engineering. Upon graduation in December, 1981, he will be reassigned to the Air Force Systems Command's Space Division at Los Angeles AFS, Los Angeles, California.

G.S. Yeakel and the former Donna Frey of Orefield, Pennsylvania were married on January 3, 1981.

Permanent Address: 12 East Elm Street
Emmaus, PA 18049

UNCLASSIFIED

SECURITY CLASSIFICATION OF THIS PAGE (When Data Entered)

REPORT DOCUMENTATION PAGE		READ INSTRUCTIONS BEFORE COMPLETING FORM
1. REPORT NUMBER AFIT/GA/AA/SID-12	2. GOVT ACCESSION NO. AD A111 261	3. RECIPIENT'S CATALOG NUMBER
4. TITLE (and Subtitle) ACTIVE CONTROL OF LINEAR PERIODIC SYSTEMS	5. TYPE OF REPORT & PERIOD COVERED M S Thesis	6. PERFORMING ORG. REPORT NUMBER
7. AUTHOR(s) Glenn S. Yeakel, 1Lt, USAF	8. CONTRACT OR GRANT NUMBER(s)	10. PROGRAM ELEMENT, PROJECT, TASK AREA & WORK UNIT NUMBERS
9. PERFORMING ORGANIZATION NAME AND ADDRESS Air Force Institute of Technology (AFIT/EN) Wright-Patterson AFB, OH 45433	12. REPORT DATE December 1981	13. NUMBER OF PAGES 108
11. CONTROLLING OFFICE NAME AND ADDRESS	15. SECURITY CLASS. (of this report) Unclassified	15a. DECLASSIFICATION DOWNGRADING SCHEDULE
14. MONITORING AGENCY NAME & ADDRESS (if different from Controlling Office)	16. DISTRIBUTION STATEMENT (of this Report) Approved for public release; distribution unlimited	
17. DISTRIBUTION STATEMENT (of the abstract entered in Block 20, if different from Report) Air Force Institute of Technology (ATC) 21773 OH 45433		
18. SUPPLEMENTARY NOTES Approved for public release; IAW AFR 190-17 Frederic Lynch, Major, USAF, Director of Information		
19. KEY WORDS (Continue on reverse side if necessary and identify by block number) Floquet Theory Modal Control Active Control Satellite Attitude Control Periodic Systems		
20. ABSTRACT (Continue on reverse side if necessary and identify by block number) The linearized equations describing the attitude motion of two generic satellite cases are developed. In both cases, the symmetric satellite in an elliptical orbit and an unsymmetric satellite in a circular orbit, the linearized equations are periodic. Using Floquet theory, the stability of the attitude motion for several satellite designs is checked. For satellites with unacceptable attitude stability, an active control scheme utilizing modal control design techniques is developed. (continued)		

DD FORM 1473

1 JAN 73

EDITION OF 1 NOV 65 IS OBSOLETE

UNCLASSIFIED

SECURITY CLASSIFICATION OF THIS PAGE (When Data Entered)

UNCLASSIFIED

SECURITY CLASSIFICATION OF THIS PAGE(When Data Entered)

With this control scheme, various satellite test cases are stabilized and the results are verified via a digital simulation of the satellite attitude motion.

UNCLASSIFIED

SECURITY CLASSIFICATION OF THIS PAGE(When Data Entered)

**DATE
FILMED**

3-8